Pergamon

Topology Vol. 33, No. 3, pp. 525–556, 1994

0040-9383/94.$7.00 + 0.00

SPECIAL POSITIONS FOR ESSENTIAL TORI IN LINK COMPLEMENTS

JOAN S. BIRMAN† and WILLIAM W. MENASCO‡

(*Received* 15 *September* 1991; *in revised form* 17 *April* 1993)

INTRODUCTION

THE decomposition of links into non-split components, by cutting along essential 2-spheres, is a fundamental step in any attempt to understand the link problem. In an earlier paper [2] the authors studied that problem from the point of view of braid theory. A somewhat more subtle decomposition of a link complement involves splitting along essential tori. By a fundamental theorem which is due to Alexander (see p. 107 of [5]) every embedded torus $\mathbf{T}$ in S^3 is the boundary of a solid torus $\mathbf{V}$ on at least one side. The solid torus $\mathbf{V}$ may, however, be knotted, and this makes the study of embedded tori much more difficult than embedded 2-spheres, since the latter cannot be knotted. The first major attempt to understand embedded tori in link complements was a groundbreaking paper by Schubert [6]. The seminal role which is played in the topology and geometry of link complements by embedded tori was later underscored in the important work of Jaco and Shalen [3], Johansson [4] and Thurston [7], who showed that if M^3 is a 3-manifold, then there is a finite collection Ω of essential, non-peripheral tori $\mathbf{T}_1,\ldots,\mathbf{T}_q$ in M^3 such that each component of M^3 split open along the tori in Ω is either Seifert-fibered or hyperbolic. Our goal in this paper is to apply the techniques of [2] to the study of essential tori in link complements.

Let λ be a link type in S^3, with representative L. A torus $\mathbf{T}$ in $S^3-\mathbf{L}$ is *essential* if it is incompressible, and *peripheral* if it is parallel to the boundary of a tubular neighborhood of $\mathbf{L}$. A link type λ is simple if every essential torus in its complement is peripheral, otherwise non-simple. Satellite links (defined below) are a special case of non-simple links.

To describe our results, assume that $\mathbf{L}$ is a closed n-braid representative of λ, with braid axis $\mathbf{A}$. The axis $\mathbf{A}$ is unknotted, so $S^3-\mathbf{A}$ is fibered by open discs $\{\mathbf{H}_\theta;\ \theta\in[0,2\pi]\}$. It will be convenient to think of $\mathbf{A}$ as the $\mathbb{Z}$-axis in $\mathbb{R}^3$, and the fibers $\mathbf{H}_\theta$ as half-planes at polar angle θ. Then $\mathbf{A}$ and the half-planes $\mathbf{H}_\theta$ serve as a "coordinate system" in $\mathbb{R}^3$ which can be used to describe both $\mathbf{L}$ and $\mathbf{T}$. We call our canonical embeddings types **0**, **1** and **k**, where in the latter case k is an integer ≥ 2. Type **0** will be familiar to most readers, but types **1** and **k** do not appear to have been noticed before this as general phenomena:

Type **0.** The torus $\mathbf{T}$ is the boundary of a (possibly knotted) solid torus $\mathbf{V}$ in S^3, whose core is a closed braid with axis $\mathbf{A}$. The link $\mathbf{L}$ is also a closed braid with respect to $\mathbf{A}$, part of it being inside $\mathbf{V}$ and part of it (possibly empty) outside. The torus $\mathbf{T}$ is transverse to every fiber $\mathbf{H}_\theta$ in the fibration of $S^3-\mathbf{A}$, and intersects each fiber in a meridian of $\mathbf{V}$. It is foliated by

†Partially supported by NSF Grant DMS-92-06584 and by the US-Israel Binational Foundation Grant 89-000302-2.
‡Partially supported by NSF grant DMS-92-00881.

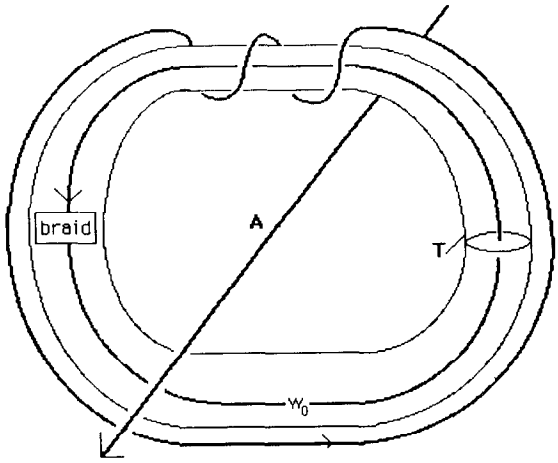

Fig. 1.

these meridian circles. An example is given in Fig. 1. In this example (and in all other braid diagrams in this paper) the braid strands are to be regarded as being weighted by arbitrary positive integer weights w_i, where weight w_i means "replace the single strand by w_i parallel strands". Notice that the axis **A** does not intersect **V**.

Type **1.** Choose a 2-sphere S which is pierced twice by **A** and has a standard north-south foliation. Choose two points of $S \backslash S \cap \mathbf{A}$, and join them by an arc α, chosen so that interior of α intersects fibers of **H** transversally. The torus obtained by tubing S to itself along a neighborhood of α, is a type **1** torus. An example is given in Fig. 2. The axis pierces **T** twice in the "sphere part" of **T**. In general the "tube part" of **T** could go around **A** several times as a braided tube. The axis **A** intersects the obvious solid torus **V** in a single arc.

Type **k** ($k \geq 2$). The torus **T** is made up of $k \geq 2$ cylinders which are glued together in a cycle. The core of the ith cylinder is an arc α_i which lies entirely in a fiber of **H** and has its endpoints on **A**. Thus each cylinder intersects **A** twice, and $|\mathbf{T} \cap \mathbf{A}| = 2k$. An example (for $k = 2$) is given in Fig. 3. In this example **T** bounds a visible unknotted solid torus **V**, but in general **V** will be knotted. (Peek ahead to Fig. 8 for an example where the arcs $\alpha_1, \ldots, \alpha_k$ which are the cores of the cylinders fit together to give the trefoil knot.) In every case $\mathbf{A} \cap \mathbf{V}$ will be a union of k unknotted, unlinked, disjoint arcs.

If we begin with an arbitrary closed braid representative **L**, then the tori $\mathbf{T}_1, \ldots, \mathbf{T}_q$ which occur in the Jaco–Shalen–Johansson decomposition will in general not be isotopic in the complement of **L** to tori of types **0**, **1** and **k**. However, if we modify **L** in an appropriate way, it may be possible to isotope them into the standard position. We will prove that the modifications which are needed are a finite sequence of "exchange moves", where an *exchange move* is defined pictorially by Fig. 4. Notice that exchange moves take closed n-braid representatives of λ to other closed n-braids. To set the stage for our work here, we note that in [2] we showed that every closed n-braid representative of a prime or split link was exchange-equivalent to a closed n-braid representative which is "obviously split or composite". Our principal result is that, up to exchanges, every torus in the Jaco–Shalen–Johansson decomposition may be assumed to be embedded in one of our three canonical ways:

THEOREM 1. *Let* $\Omega = \{\mathbf{T}_1, \ldots, \mathbf{T}_q\}$ *be the finite collection of tori in the Jaco–Shalen–Johansson decomposition of* $S^3 - \mathbf{L}$. *Then there is a finite sequence of n-braids:*

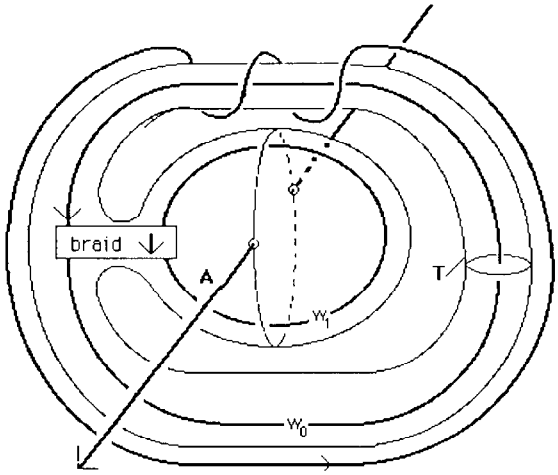

Example of type **1** embedding

Fig. 2.

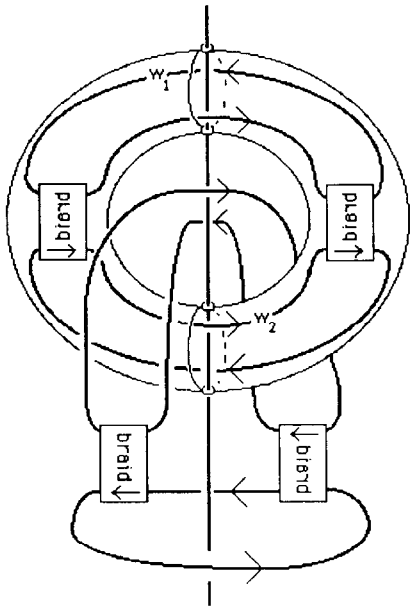

Example of a type **k** embedding (k=2)

Fig. 3.

$$\mathbf{L} = \mathbf{L}_1 \to \mathbf{L}_2 \to \ldots\ldots \to \mathbf{L}_m = \mathbf{L}^*$$

such that each $\mathbf{L}_{i+1}$ *is obtained from* $\mathbf{L}_i$ *by an exchange move together with an isotopy in the complement of* $\mathbf{A}$, *such that in the braid fibration associated with* $\mathbf{L}^*$ *each torus in the modified collection* $\mathbf{\Omega}^*$ *is isotopic in the complement of* $\mathbf{L}^* \cup \mathbf{A}$ *to a torus of type* $\mathbf{0}$, $\mathbf{1}$ *or* $\mathbf{k}$ ($k \geq 2$).

Implicit in Theorem 1 is a description of all non-simple links, via their closed braid representatives. We are able to make this explicit in the special cases of links of braid index 3 and 4. Let σ_i denote an elementary braid in which the ith braid strand is interchanged with the $i + 1$st.

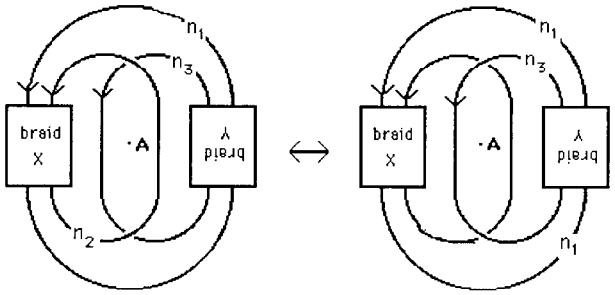

The Exchange Move

Fig. 4.

COROLLARY 1. *Let* **L** *be a closed* 3*-braid representative or a prime link of braid index* 3, *and let* **T** *be a nonperipheral essential torus in* S^3–**L**. *Then* **T** *has a type* **0** *embedding, and* **L** *is conjugate to*:

$$(\sigma_2)^p(\sigma_1\sigma_2^2\sigma_1)^q, \quad \text{where } |p| \geq 2, \quad |q| \geq 1.$$

Let σ_{ij}, denote an elementary braid in which the ith and jth strands exchange positions, the jth crossing over the ith, and both passing in front of all intermediate braid strands as they do so.

COROLLARY 2. *Let* **L** *be a* 4*-braid representative of a prime link of braid index* 4, *and let* **T** *be a nonperipheral essential torus in* S^3–**L**. *Then after a series of exchange moves, the conjugacy class of* **L** *and type of* **T** *may be assumed to be one of the following,*

Type **0.** $(\sigma_1)^p(\sigma_3)^q(\sigma_2\sigma_1\sigma_3\sigma_2)^r$, where $|p| > 0$, $|q| > 0$, and $|r| \geq 2$, or

$\beta(\sigma_3\sigma_2\sigma_1^2\sigma_2\sigma_3)^p$, where $|p| \geq 1$, for any 3-braid $\beta = W(\sigma_1, \sigma_2)$, or

$(\sigma_2)^p(\sigma_1\sigma_2^2\sigma_1)^q(\sigma_3\sigma_2^2\sigma_3)^r$, where $|p|, |q|, |r| > 0$.

Type **1.** $\beta(\sigma_1\sigma_2^2\sigma_1)^p$, $|p| \geq 1$, for any 3-braid $\beta = W(\sigma_2, \sigma_3)$,

Type **2.** $(\sigma_{13})^p(\sigma_{24})^r(\sigma_{13})^q(\sigma_{24})^s$, where $|p|, |q|, |r|, |s| > 0$.

Our second set of results concerns numerical data which appears as a result of the partial normal forms of Theorem 1. Let **L** be a link which is represented as a closed braid, relative to a choice of braid axis **A** and fibration **H**. Suppose that there is an essential, non-peripheral torus **T** in S^3–**L**. By a well-known theorem of Alexander, **T** bounds a solid torus **V** on at least one side. In general, the braid axis **A** will intersect **V** in a finite family of disjoint arcs, and some features of the closed braid representation of **L** can be deduced by investigating the relative local positions of $\mathbf{L} \cap \mathbf{V}$ and $\mathbf{A} \cap \mathbf{V}$ in **V**.

THEOREM 2.

(i) *Assume that* **T** *has a type* **0**, **1** *or* **k** *foliation. Let* **V** *be the solid torus which* **T** *bounds. Then* $\mathbf{A} \cap \mathbf{V}$ *is a union of* 0, 1 *or* $k \geq 2$ *arcs, according as* **T** *has a type* **0**, **1** *or* **k** *foliation, where in the situation of type* **0**, *if* **T** *bounds on both sides we choose* **V** *so that* $\mathbf{A} \cap \mathbf{V}$ *is empty.*

(ii) *The inclusion of* $(\mathbf{L} \cup \mathbf{A}) \cap \mathbf{V}$ *in* **V** *in the* 3 *cases is as depicted in Fig.* 5. *Each component of* $\mathbf{A} \cap \mathbf{V}$ *is illustrated in the projection as a heavy black dot, and* $\mathbf{L} \cap \mathbf{V}$ *wraps*

around these arcs to give "local" braid diagrams. The weights $w_0, w_1, \ldots, w_k$ *are the number of braid strands of* **L** *in the local pictures in Fig.* 5 *(also see the examples in Figs* 1, 2, 3).

(iii) *If it should happen that* **V** *is unknotted, so that* $\mathbf{V}' = S^3 - \mathbf{V}$ *is also a solid torus, then a symmetric description holds for the inclusion of* $(\mathbf{L} \cup \mathbf{A}) \cap \mathbf{V}'$ *in* $\mathbf{V}'$, *for types* **1** *and* **k**.

As an application of Theorem 2 we consider the special case of satellite links. Let $\mathbf{V}_m$ be a standard model for an embedded solid torus in R^3, say a torus of revolution. Let **M** be a non-trivial knot or link which is embedded in a geometrically essential manner in $\mathbf{V}_m$, i.e. **M** meets every meridian disc of $\mathbf{V}_m$ non-trivially, also **M** is not isotopic to the core of $\mathbf{V}_m$. Let **C** be any non-trivial knot in R^3, and let $\mathbf{V}_c$ be a solid torus neighborhood of **C**. Let h: $\mathbf{V}_m \to \mathbf{V}_c$ be a homeomorphism, and let $\mathbf{L} = h(\mathbf{M})$. Then **C** is a *companion* of the *satellite* link **L**, and **M** is the *model* for **L**. Notice that satellite knots always have an incompressible torus in their complement, i.e. $\partial \mathbf{V}_c$. The fact that, by hypothesis, **M** is not isotopic to the core of $\mathbf{V}_m$ ensures that $\mathbf{T}_c = \partial \mathbf{V}_c$ is not peripheral. The fact that, by hypothesis, **C** is knotted ensures that $\mathbf{T}_c$ does not bound a solid torus on both sides.

If **L** represents a link type, its *braid index* $b(\mathbf{L})$ is the smallest integer n such that **L** is isotopic to an n-braid. Our application is a new proof and generalization of a theorem of Schubert [6] about the braid index of satellite links. Recall that in Fig. 5 and also in the

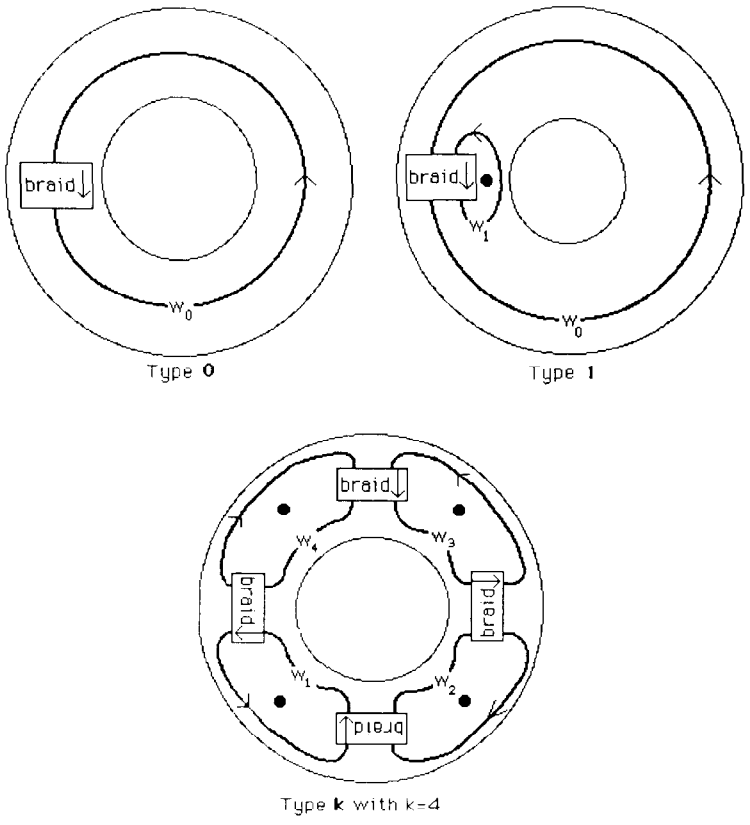

$(\mathbf{L} \cup \mathbf{A}) \cap \mathbf{V}$ for the three types of embeddings of $\mathbf{T} = \partial \mathbf{V}$

Fig. 5.

examples in Figs 1, 2, 3 we defined the weights:

w_0 in the case where $\mathbf{T}_c$ has a type **0** embedding,
w_0, w_1 in the case where $\mathbf{T}_c$ has a type **1** embedding, and
$w_1,\ldots,w_k$ in the case where $\mathbf{T}_c$ has a type **k** embedding.

COROLLARY 3. † *Let* **L** *be a satellite knot with model* **M** *and companion* **C**. *Let* $\mathbf{T}_c = \partial \mathbf{V}_c$. *Then*:

$b(\mathbf{L}) = w_0 \cdot b(\mathbf{C})$ if the embedding of $\mathbf{T}_c$ is type **0**. (cf Satz 23.2 of [6])

$b(\mathbf{L}) = w_0 \cdot b(\mathbf{C}) + w_1$ if the embedding of $\mathbf{T}_c$ is type **1**.

$b(\mathbf{L}) = w_1 + w_2 + \ldots + w_k$ if the embedding of $\mathbf{T}_c$ is type $\mathbf{k} \geq 2$.

The proof of Corollary 3 will follow directly from the machinery we develop to prove Theorems 1 and 2. We sketch it now, because it shows the usefulness of the structure provided by our "coordinate system", i.e. the braid axis and the fibers of **H**.

Proof of Corollary 3. Let $b(\mathbf{L})$ be the braid index of **L**. We choose a closed $b(\mathbf{L})$-braid structure for **L**, with axis **A**. The complement of the axis **A** is an open solid torus, which is fibered by meridian discs $\{\mathbf{H}_\theta;\ \theta \in [0, 2\pi]\}$. The link **L** intersects each fiber $\mathbf{H}_\theta$ of **H** in $b(\mathbf{L})$ points, which we refer to as "dots". Our task is to count the dots. By Theorem 1 we may assume that T_c has an embedding of type **0**, **1** or **k** relative to the fibers $\{\mathbf{H}_\theta;\ \theta \in [0, 2\pi]\}$ in our braid structure. This means that if $\mathbf{H}_\theta$ is non-singular, then $\mathbf{T}_c \cap \mathbf{H}_\theta$ will be a family of arcs and circles. The idea is to choose $\mathbf{H}_\theta$ so that the arcs and circles subdivide the dots into groups which are convenient for counting purposes. See Fig. 6.

Type **0**. There are no singular fibers, and any $\mathbf{H}_\theta$ will do. The fact that the braid index of **L** is minimal implies that the core of $\mathbf{V}_c$ must be a closed $b(\mathbf{C})$-braid with respect to **A**. The intersections of $\mathbf{T}_c$ with $\mathbf{H}_\theta$ will therefore be a collection of $b(\mathbf{C})$ circles. Each circle bounds a disc d_c in $\mathbf{H}_\theta$, and d_c contains w_0 dots. Thus $b(\mathbf{L}) = w_0 \cdot b(\mathbf{C})$, as claimed.

Type 1. The incompressible torus which is being studied has a natural decomposition as a union of a single punctured 2-sphere S with a braided tube attached to it. The sphere and tube are joined along an annulus A. We choose our fiber $\mathbf{H}_\theta$ so that it does not meet the annulus. With this choice $\mathbf{T}_c \cap \mathbf{H}_\theta$ will consist of a single arc and n circles $c_1,\ldots,c_n$, if **C** is represented as an n-braid. The arc bounds a half-disc which contains w_0 dots. The total number of dots will be $(w_0 \cdot n + w_1)$. The integers w_0 and w_1 are both invariants of the model **M**, thus the braid index of the satellite will be minimized when the braid index of the companion is minimized. Thus $b(\mathbf{L}) = w_0 \cdot b(\mathbf{C}) + w_1$, as claimed.

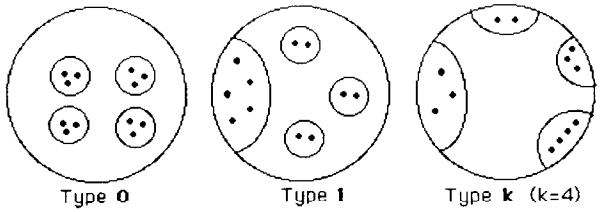

Intersections of T and L with a
special non-singular fiber $\mathbf{H}_\theta$ of **H**

Fig. 6.

†See the note, added in proof, at the end of the paper.

Type **k**. The incompressible torus which is being studied has a natural decomposition as a union of k twice-punctured spheres $S_1, \ldots, S_k$ joined up in a cycle by annuli $A_1, \ldots, A_k$. We choose $\mathbf{H}_\theta$ so that it does not intersect the annuli. With this choice $\mathbf{T}_c \cap \mathbf{H}_\theta$ will consist of exactly k arcs, $b_1, \ldots, b_k$, where the ith arc cuts off a half-disc which does not contain any other b_j. (Every non-singular fiber intersects $\mathbf{T}_c$ in a family of k arcs, but in general both half-discs determined by a typical arc b_i will contain other arcs b_j). The half-disc contains w_i dots. Thus $b(\mathbf{L}) = w_1 + w_2 + \ldots + w_k$, as claimed. ‖

A doubled knot **L** is a satellite knot which is based upon the model which is illustrated in the top right sketch in Fig. 7. Its companion is an arbitrary non-trivial knot. In the example in Fig. 7 it is a trefoil. Our final result concerns the essential torus $\mathbf{T}_c$ in the case when **L** is a doubled knot.

COROLLARY 4. *Let* **L** *be a doubled knot with companion* **C**. *Assume that* **L** *is represented in any way as a closed braid. Then after a series of exchange moves the essential torus* $\mathbf{T}_c = \partial \mathbf{V}_c$ *in* $S^3 - \mathbf{L}$ *will have a type* **k** *embedding.*

Proof of Corollary 4. Let $\mathbf{V}_c$ be a tubular neighborhood of the companion, so that $\mathbf{V}_c$ contains **L**. Let $\mathbf{T}_c = \partial \mathbf{V}_c$. Notice (consult the model) that **L** intersects each meridian disc of

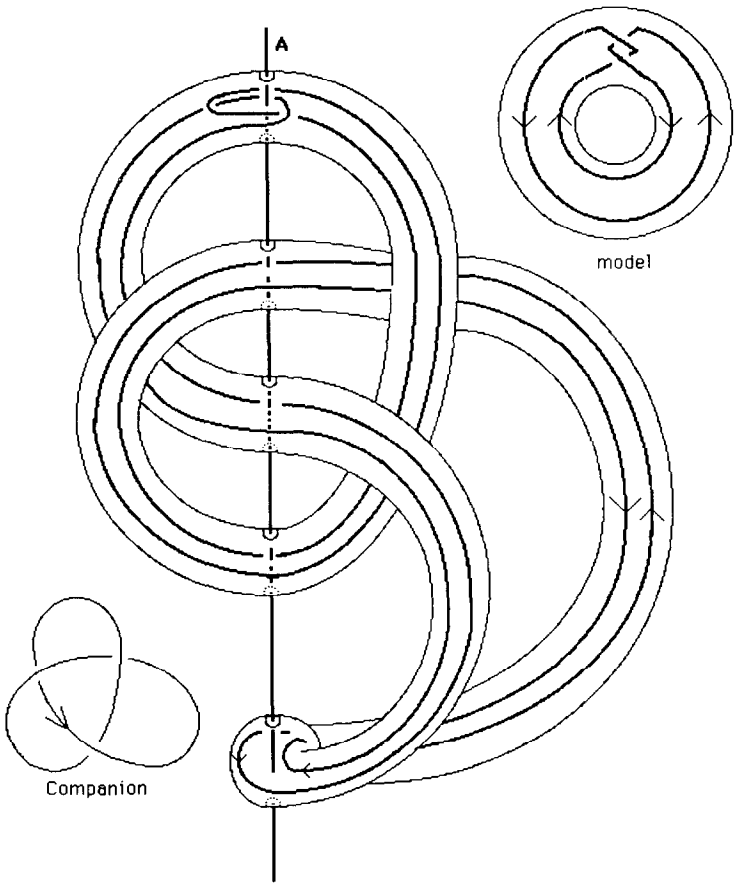

Fig. 7.

$\mathbf{V}_c$ zero times algebraically. Choose a closed braid structure with axis **A** and fibration **H** for **L**. By Theorem 1, we may assume without loss of generality that $\mathbf{T}_c$ has an embedding of type **0**, **1** or **k** relative to **H**. However, from Fig. 5 we conclude that $\mathbf{T}_c$ cannot be type **0** or **1**, because in each of those cases there is a meridian disc of $\mathbf{V}_c$ which intersects **L** with non-zero algebraic intersection number. Thus T_c must have a type **k** embedding. ‖

Examples of Corollary 4 are interesting and subtle. Figure 7 gives one, when **L** is a double of the trefoil knot **C**. In this example $k = 5$. This example illustrates that the formula in Corollary 3 for $b(\mathbf{L})$ in the case of type **k** embeddings is more complicated than it appears to be, because in Fig. 5 we are looking at the inclusions of $(\mathbf{L} \cup \mathbf{A}) \cap \mathbf{V}_c$ in $\mathbf{V}_c$, and this contains more structure than $\mathbf{L} \cap \mathbf{V}_c$, which is homeomorphic to $\mathbf{M} \cap \mathbf{V}_m$. For example, in the situation of the doubled knot which is illustrated in Fig. 7 there is a model **M** which contains 2 blocks. However, when we add **A** we see that we need 5 braid blocks, not 2. The additional blocks correspond to additional braid crossings which cancel as braid crossings, but which are needed in order to give the correct embedding of $\mathbf{L} \cup \mathbf{A}$ in $\mathbf{V}_c$.

The structure which is imposed by doubling a knot is so very far away from the structure imposed by a braid axis, that one would not expect that anything at all could be said about the braid representatives of doubled knots. However, the work we have done suggests a conjecture:

Conjecture: Let $\mathbf{D}(\mathbf{C})$ be a doubled knot with companion **C**. By Corollary 4 the natural torus $\mathbf{T}_c = \partial \mathbf{V}_c$ in $S^3 - \mathbf{D}(\mathbf{C})$ has a type **k** embedding. The example in Fig. 7 then suggests that when $\mathbf{D}(\mathbf{C})$ is represented as a closed braid with a minimum number of braid strands, its companion **C** will have a projection which exhibits it as a union of k unknotted and unlinked arcs $\alpha_1, \ldots, \alpha_k$, each of which has its endpoints on **A**. See Fig. 8 for an example, in the case of the trefoil. The smallest integer k such that **C** can be so-represented is (by definition) a numerical knot invariant $k(\mathbf{C})$ of the knot type of **C**. It is reasonable to conjecture that the braid index of $\mathbf{D}(\mathbf{C})$ is determined by the integer $k(\mathbf{C})$ and the framing. The invariant $k(\mathbf{C})$ seems not to have been noticed.

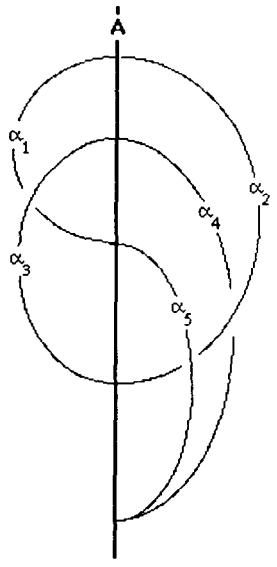

Fig. 8.

The organization of this paper is as follows. In §1 we introduce our basic machinery, which will involve the study of certain foliations of essential tori. Tori which admit a circular foliation will be seen to have an embedding of type **0**, but the other cases are more complicated. In §2 we standardize the foliations for tori which have tilings, and show that after this standardization the embedding is type **k**. In §3 we standardize the mixed foliations, and show that (after further modifications) they have type **1** embeddings. In §4 we use all of this to prove Theorem 1, Corollaries 1 and 2 and Theorem 2.

§1. FOLIATIONS ON TORI

The techniques used in this paper are related to techniques used in [2]. In this section we give a quick review of the relevant material, with references, as we need them, in lieu of repeating details of arguments which are published elsewhere.

Our work begins with a non-simple link type λ, a closed n-braid representative $\mathbf{L}$, and an essential non-peripheral torus $\mathbf{T}$ in $S^3 - \mathbf{L}$. The closed braid structure is defined relative to a braid axis $\mathbf{A}$ and a choice $\mathbf{H}$ of fibration of $S^3 - \mathbf{A}$ by meridian discs $\{\mathbf{H}_\theta; \theta \in [0, 2\pi]\}$. The intersection of the $\mathbf{H}_\theta$'s with $\mathbf{T}$ induce a foliation of $\mathbf{T}$. In this section we begin to standardize the foliations.

LEMMA 1. *We may assume that*:

(i) *The intersections of* $\mathbf{A}$ *with* $\mathbf{T}$ *are finite in number and transverse. Also, if* $p \in \mathbf{A} \cap \mathbf{T}$, *then* p *has a neighborhood on* $\mathbf{T}$ *which is radially foliated by its arcs of intersection with fibers of* $\mathbf{H}$.

(ii) *All but finitely many fibers* $\mathbf{H}_\theta$ *of* $\mathbf{H}$ *meet* $\mathbf{T}$ *transversally, and those which do not (the singular fibers) are each tangent to* $\mathbf{T}$ *at exactly one point in the interior of both* $\mathbf{T}$ *and* $\mathbf{H}_\theta$. *Moreover, the tangencies are local maxima or minima or saddle points.*

Proof. Use general position. ∎

A singular leaf in the foliation of $\mathbf{T}$ *will be one which contains a point of tangency. All other leaves are non-singular. It follows from* (ii) *that*:

(iii) *Each non-singular leaf is either an arc or a simple closed curve.*

(iv) *A singular fiber contains exactly one singular point.*

(v) *Each singular point is either a center or a saddle.*

We refer to the leaves of the foliation of $\mathbf{T}$ as **b**-*arcs* and **c**-*circles*. Each **b**-arc and each **c**-circle lies in both $\mathbf{T}$ and in some fiber $\mathbf{H}_\theta$ of $\mathbf{H}$. A **b**-arc b is *essential* if both sides of $\mathbf{H}_\theta$ split along b are pierced by $\mathbf{L}$. A **c**-circle, c in $\mathbf{T} \cap \mathbf{H}_\theta$, is *essential* if c bounds a subdisc d_c of $\mathbf{H}_\theta$ such that $d_c \cap \mathbf{L}$ is nonempty.

LEMMA 2. *Assume that* $\mathbf{T}$ *satisfies* (i)–(v) *and has* **b**-*arcs or* **c**-*circles in the induced foliation. Then we may replace* $\mathbf{T}$ *with an essential torus,* $\mathbf{T}'$, *such that the foliation of* $\mathbf{T}'$ *also satisfies* (i)–(v) *and*:

1. *All* **b**-*arcs are essential.*
2. *All* **c**-*circles are essential.*
3. *Any* **c**-*circle in the foliation is homotopically non-trivial on* $\mathbf{T}$.

Moreover, if $\mathbf{L}$ *is not a split link then* $\mathbf{T}'$ *is isotopic to* $\mathbf{T}$.

Proof

1. Suppose that b is an inessential **b**-arc in a fiber $\mathbf{H}_\theta$ of **H**. Then one of the sides of $\mathbf{H}_\theta$ split along b is a disc d_b which is not pierced by **L**. Without loss of generality we may assume that b is innermost. We may then push **T** across **A** in a regular neighborhood of d_b in 3-space to remove the **b**-arc from $\mathbf{H}_\theta$ and all nearby fibers.

2. To show that we can remove inessential **c**-circles we reason as Bennequin did, in [1].

3. Suppose that c is an essential **c**-circle in a fiber $\mathbf{H}_\theta$ of **H**. We may assume without loss of generality that c is inner-most in $\mathbf{H}_\theta$. Then c bounds a sub-disc d_1 of $\mathbf{H}_\theta$, which is punctured by **L** algebraically non-zero times. If c is homotopically trivial on **T** then c bounds a sub-disc of **T**, d_2. We can construct a 2-sphere by gluing d_1 to d_2 along c. But this will be punctured algebraically non-zero times of **L**, which is impossible for a 2-sphere in 3-space. Thus, c must be homotopically non-trivial on **T**. ‖

We now consider the different types of singularities which can occur in the foliation. Since there are only two types of leaves in the foliation there are at most three possible types of singularities, which may be described as types **bb**, **bc** and **cc**, according as the leaves which are surgered are both type **b**, types **b** and **c**, or both type **c**.

LEMMA 3. *Singularities of type* **cc** *do not occur.*

Proof. A surgery between two **c**-circles will produce a homotopically trivial simple closed curve, violating assertion 3 of Lemma 2. ‖

We restrict our attention, temporarily, to the situation where every leaf in the foliation of **T** is a **b**-arc. This is exactly the situation which was studied in [2], for a foliated essential 2-sphere **X** in a link complement. It was shown that in this situation there is a natural foliated cell-decomposition of **X**. The 0-cells of the decomposition are the points of $\mathbf{A} \cap \mathbf{X}$, and the 2-cells are foliated squares, each of which contains exactly one **bb**-singularity. We call these squares **bb-tiles**. The 1-cells are any convenient choice of non-singular **b**-arcs in the foliation of **X** which divide **X** into **bb**-tiles. See Fig. 9. The description of this cell decomposition goes through in exactly the same way if we replace the 2-sphere **X** by our essential, non-peripheral torus **T**. There is a natural foliated cell-decomposition of **T**, as before, and each 2-cell has 4 sides and contains a single **bb**-singularity.

A related situation exists when both **bb**- and **bc**-singularities occur, only now we must decompose **T** along a finite collection of non-singular **b**-arcs and **c**-circles into a union of **bb**-tiles and **bc**-annuli, depicted in Fig. 9. Each **bc**-annulus contains two points of $\mathbf{A} \cap \mathbf{T}$ in its boundary, and exactly one singularity of the foliation in its interior. The singularity is type **bc**. This leads us to the following definitions:

If the foliation of **T** consists entirely of **c**-circles, with no singularities, then **T** has a *circular foliation.*

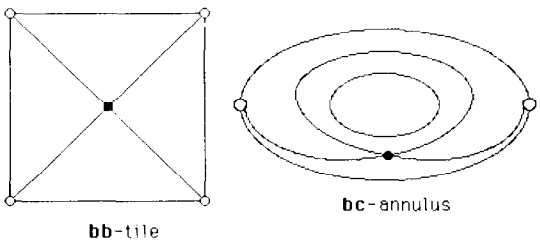

Fig. 9.

If the leaves in the foliation of $\mathbf{T}$ include both **b**-arcs and **c**-circles, so that the singularities include both **bb**- and **bc**-singularities, we say that $\mathbf{T}$ has a *mixed foliation.*

If every non-singular leaf in the foliation of $\mathbf{T}$ is a **b**-arc, and every singularity is a **bb**-singularity, we say that $\mathbf{T}$ admits a *tiling.*

Now observe that if we have a collection Ω of finitely many tori instead of just one torus, all of the modifications so far may be done on them, one at a time. Therefore, using the notation just introduced, we may put together Lemmas 1–3 to obtain:

LEMMA 4. *We may assume that each torus $\mathbf{T}_i$ in Ω has either a circular foliation or a mixed foliation or a tiling. Moreover, if the foliation is circular, then $\mathbf{T}_i$ has a type* **0** *embedding.*

Proof. Everything except the last assertion has been proved. So, assume that $\mathbf{T}_i$ admits a circular foliation. There are no singularities in the foliation of $\mathbf{T}_i$ and every leaf c_θ is a circle. Since each c_θ lies in a fiber $\mathbf{H}_\theta$, it bounds a disc d_θ in $\mathbf{H}_\theta$. These discs sweep out a solid torus $\mathbf{V}_i$ and every leaf in the foliation of $\mathbf{T}_i$ is a meridian of $\mathbf{V}_i$. The embedding is type **0**. ‖

§2. TORI WHICH ADMIT TILINGS

Our goal in this section is to prove that if a torus has a tiling, we may modify it to one which has a "standard" tiling. After the tiling is standardized we will be able to prove that the embedding is type **k**, where $k \geq 2$.

Let $\mathbf{T}$ be a torus which admits a tiling. The *valence* of a vertex in the tiling of $\mathbf{T}$ is the number of tiles which meet at that vertex. Assign a positive side to $\mathbf{T}$, arbitrarily. The *sign* of a tile is $+$ (respectively minus) according as the sense of the outward pointing normal to $\mathbf{T}$ at the singular point agrees (resp. disagrees) with the sense of normal to $\mathbf{H}_\theta$ which points in the direction of increasing θ. We say that a tiling is *standard* if all of its vertices are valence 4, and if the signs of the four tiles which intersect at a common vertex are $+, -, +, -$ in that cyclic order. (We will see later that this implies much more: There is a fundamental domain for $\mathbf{T}$ which is a tiled rectangle of dimension 2 tiles by $2k$ tiles, with opposite sides identified.) Our first goal in this section is to show that after a series of exchange moves the tilings of Lemma 4 may be modified to standard tilings. Similar work was done in [2], when we considered tilings of 2-spheres in the complement of a split link λ which is represented as a closed braid. If $\mathbf{X}$ is a surface in 3-space which admits a tiling relative to $\mathbf{H}$, we define the *complexity* $C(\mathbf{X}, \mathbf{H})$ of the tiling to be the pair (V, R), where V is the number of vertices and R the number of tiles. We say that $C(\mathbf{X}', \mathbf{H}') = C(\mathbf{X}, \mathbf{H})$ if $(V', R') < (V, R)$ using lexicographical ordering. If we had realized when we wrote [2] that we would need Lemma 3 of that paper for this paper, we would have stated it as follows:

LEMMA 5. (Lemma 3 of [2], restated). *Let $\mathbf{X}$ be a surface which is in the complement of $\mathbf{L}$. Assume that $\mathbf{X}$ has a tiling, with complexity $C(\mathbf{X}, \mathbf{H})$. Suppose there is a foliated subset $\mathbf{N}_0$ of $\mathbf{X}$ which is the star of a vertex p of valence $v \geq 3$. Suppose that there are adjacent singularities* **s** *and* **s**′ *in $\mathbf{N}_0$ which have the same sign. Then there is an isotopy of $\mathbf{X}$ in the complement of $\mathbf{L}$ to a surface $\mathbf{X}'$, with $C(\mathbf{X}', \mathbf{H}) = C(\mathbf{X}, \mathbf{H})$, such that the tiling of $\mathbf{X}'$ is identical to that of $\mathbf{X}$ everywhere except in $\mathbf{N}_0$, and in the new tiling the valence of p is reduced to $v - 1$. Moreover, the isotopy is supported in a disc neighborhood $\mathbf{N}$ in $\mathbf{N}_0$ of an arc μ which joins* **s** *to* **s**′ *in $\mathbf{N}$, chosen so that μ crosses only non-singular leaves, and crosses each such leaf transversally.*

Proof. The assertion can be understood intuitively with the help of Fig. 10. The top picture shows $\mathbf{N}_0$ embedded in 3-space. Fibers of $\mathbf{H}$ are horizontal planes. The isotopy of $\mathbf{X}$ may be visualized as a coalescing of the two singularities to a single monkey saddle, and then a splitting apart in a new way. The bottom picture shows the changes in the foliation of $\mathbf{N}_0$ as the singularities coalesce and split apart again, in the case when $\mathbf{N}_0$ is a union of two adjacent **bb**-tiles.

See the proof of Lemma 3 of [2] for details. ‖

LEMMA 6. *Suppose that* $\mathbf{T}$ *has a tiling which is induced by the fibration* $\mathbf{H}$ *of* $S^3 - \mathbf{A}$. *Then,*

(i) *If there is a vertex* p *of valence* v *in the tiling of* $\mathbf{T}$ *such that there are adjacent tiles meeting at* p *which have the same sign, then there is an isotopy of* $\mathbf{T}$ *in the complement of* $\mathbf{L}$ *to a tiled torus* $\mathbf{T}'$ *such that* $C(\mathbf{T}', \mathbf{H}) = C(\mathbf{T}, \mathbf{H})$, *and in the tiling of* $\mathbf{T}'$ *the vertex* p *has valence* $v - 1$.

(ii) *If there is a vertex of valence* 2 *or* 3 *in the tiling of* $\mathbf{T}$, *the closed braid* $\mathbf{L}$ *admits an exchange. After the exchange there will be a new torus* $\mathbf{T}'$ *with a tiling such that* $C(\mathbf{T}', \mathbf{H}) < C(\mathbf{T}, \mathbf{H})$.

Proof.

(i) This is a consequence of Lemma 5 above.

(ii) First suppose that there is a vertex of valence 3 in the tiling of $\mathbf{T}$. Either all of the tiles have the sign, or two of them have one sign and the third the opposite sign. Thus we may always find a pair of adjacent tiles with the same sign. By Lemma 5 above there is then an

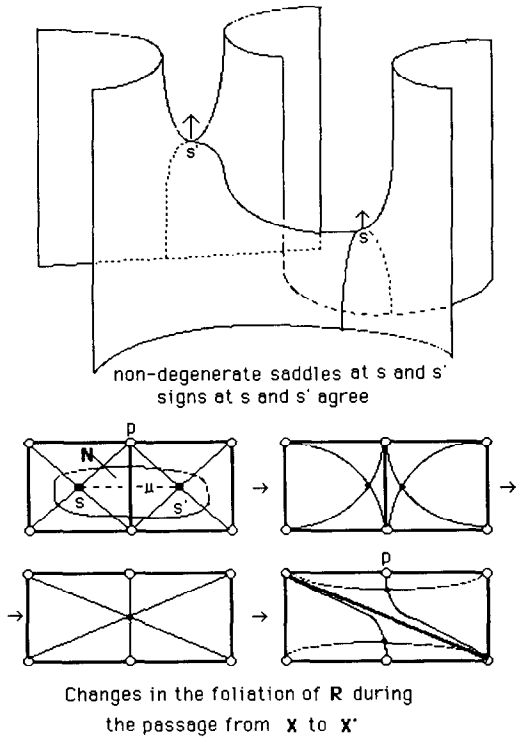

Fig. 10.

isotopy of **T** to a new torus **T'** such that the tiling of **T'** has a vertex of valence 2, also $C(\mathbf{T}', \mathbf{H}) = C(\mathbf{T}, \mathbf{H})$. We may thus assume that the tiling of **T** contains a vertex of valence 2. This is the situation which was considered in Lemma 4 of [2]. The argument in Lemma 4 of [2] related to the situation where there is a 2-sphere **X** (rather than an essential torus **T**) in the complement of **L**, however it makes no use at all of the global topology of **X**, and the arguments go over without any change at all when we replace **X** by **T**. By Lemma 4 of [2] we conclude that **L** admits an exchange move, and also after the exchange move **T** can be modified by isotopy to a new essential torus **T'**, such that $C(\mathbf{T}', \mathbf{H}) < C(\mathbf{T}, \mathbf{H})$. ‖

LEMMA 7. *Assume that* **T** *is a torus in the complement of a closed braid, and that* **T** *admits a tiling. Then, after a sequence of exchanges we may assume that* **T** *admits a standard tiling.*

Proof. As noted earlier, the tiling of **T** produces a natural foliated cellular decomposition of **T**. Let V, E and R be the number of 0, 1 and 2-cells. Then $V - E + R = 0$, because **T** is a torus. Since each 1-cell is the boundary of exactly two 2-cells, and each 2-cell has four 1-cells in its boundary, we have $2R = E$. Thus $2V - E = 0$. Now let $V(i)$ be the number of vertices having valence i. Since there are no vertices of valence 1, we have $V = V(2) + V(3) + V(4) + \ldots$. Since each edge has 2 vertices in its boundary we have $2E = 2V(2) + 3V(3) + 4V(4) + \ldots$. Thus

$$2V(2) + V(3) = V(5) + 2V(6) + 3V(7) + \ldots . \tag{1}$$

By equation (1), if there are any vertices having valence other than four then there must exist vertices of valence 2 or 3. It then follows from Lemma 6 that **L** admits an exchange move. After the exchange, we may eliminate two points of $\mathbf{A} \cap \mathbf{T}$. Continue in this manner until every vertex has valence 4.

Now suppose that there is a vertex p such that a pair of adjacent tiles in the cyclically ordered array of 4 tiles about p which have the same signs. By assertion (i) of Lemma 6 we may find a new fibration **H'** such that the valence of p is reduced to 3. But then, after an exchange we may reduce the complexity by eliminating two points of $\mathbf{A} \cap \mathbf{T}$. This process ends with a torus **T** which has a standard tiling. ‖

LEMMA 8. *A torus which has a standard tiling has a type* **k** *embedding.*

Proof. We are given a torus **T** which admits a standard tiling, i.e. **T** is a union of **bb**-tiles, every vertex in the tiling has valence 4, and the cyclically ordered array of signs of the four tiles which meet at each vertex are $+, -, +, -$. We will show that **T** has a type **k** embedding.

We begin our proof with an observation about the order of the vertices of a **bb**-tile around the tile boundary and along the axis **A**. Let **T** be such a tile, and let **1**, **2**, **3**, **4** be its vertices, cyclically oriented around $\partial\mathbf{T}$, as in Fig. 11. The vertices represent points where the braid axis **A** pierces the torus **T**, and we claim that the four vertices have the same cyclic order **1**, **2**, **3**, **4** (or its reverse) on **A** as on $\partial\mathbf{T}$. To see this, suppose that the arrows on the leaves of the foliation on **T** denote the sense of the flow as θ is increasing. Choose two non-singular leaves, say α and α^* which lie in the same fiber $\mathbf{H}_\theta$ of **H**, before the singularity. Since these leaves are disjoint arcs in $\mathbf{H}_\theta$, it follows that the endpoints $\mathbf{1} \cup 2$ of α cannot separate the endpoints $\mathbf{3} \cup \mathbf{4}$ of α^* on $\mathbf{A} = \partial\mathbf{H}_\theta$. So the cyclic order is either **1**, **2**, **3**, **4** or **1**, **2**, **4**, **3** or the reverse of one of these. Now choose two leaves β and β^* which are in the same fiber $\mathbf{H}_\phi$ after the singularity on **T**. Since β and β^* are disjoint arcs in $\mathbf{H}_\phi$, the endpoints $\mathbf{2} \cup \mathbf{3}$ of β cannot separate the endpoints $\mathbf{1} \cup \mathbf{4}$ of β^* on $\mathbf{A} = \partial\mathbf{H}_\phi$. But then the order must be **1**, **2**, **3**, **4** or its

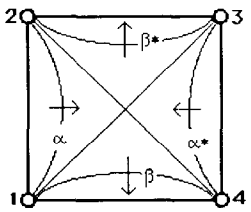

Fig. 11.

reverse, as claimed.

Our next general observation is that if V, E and F denote the number of vertices, edges and faces in the tiling, then $V = F$ and $E = 2F$. This follows from the fact that each tile has four edges and each edge is adjacent to exactly two tiles, so $E = 2F$. Then the Euler characteristic of **T** is $0 = V - E + F = V - F$, and the assertion is proved.

To continue, we assume that **T** has been cut open to a tiled fundamental domain R which is a rectangle of dimensions **k** tiles by **k**′ tiles. If **T** is a tile in R, then if we cross any edge of **T** we will encounter a tile of opposite sign, so we may assume without loss of generality that R has been chosen so that $k \geq 2$ and $k' \geq 2$. We now consider Theorem 1 in the special case when $k = k' = 2$, so $V = F = 4$. All four tiles have the same four vertices, and from this it follows (see the left picture in Fig. 12) that the cyclic order of the vertices around each is alternately **1, 2, 3, 4** and **4, 3, 2, 1**. Notice also (the left picture in Fig. 12 again) that the sense of increasing θ is clockwise about **1** and **3** and counterclockwise about **2** and **4**.

Choose four points on the oriented axis **A** and declare them to be **1, 2, 3, 4** in that order. Next, choose little disc neighborhoods of the vertices, and attach them to the axis. If the two sides of the oriented surface **T** are painted red and green, the fact that the sense of the flow is alternately clockwise and counterclockwise about **1, 2, 3, 4** shows that the axis **A** will pierce **T** from the red, green, red and green sides at **1, 2, 3, 4**.

The next step is to embed the singular leaves in 3-space. By hypothesis, the four singularities occur at four distinct values of θ. Choose four distinct fibers of **H**, say at θ_1, θ_2, θ_3 and θ_4 in that cyclic order in the fibration, and put down the pair of singular leaves (joining **1** to **3** and **2** to **4**) in each fiber. Next add an arrow at each of the four singular points pointing in the direction of increasing or decreasing θ, according as the singularity is positive or negative. See the right picture in Fig. 12. The front left and rear right tiles have positive signs and the front right and rear left ones have negative signs. The remaining regions of **T** are everywhere transverse to the leaves of the foliation and there is a unique way to attach them. This proves Lemma 8, in the case where $k = k' = 2$. Notice that in this case **T** is a union of two "tubes", each of which is made up out of two **bb**-tiles.

Our next claim is that in the general case either k or k' must be 2. We have already shown that we may assume that $k, k' \geq 2$, so to prove this assertion we assume that $k' > 2$ and $k > 2$ and arrive at a contradiction. Choose a non-singular fiber $\mathbf{H}_0$. A **b**-arc β in $\mathbf{H}_0$ will be called *innermost* if one of the sides of the axis **A** split along $\partial\beta$ contains no other points of $\mathbf{A} \cap \mathbf{T}$. Choose an innermost **b**-arc β in $\mathbf{H}_0$. Without loss of generality we may assume that β is a common edge of a pair of adjacent tiles T_1 and T_2 in the tiling of **T**, as in Fig. 13. The six vertices of $T_1 \cup T_2$ are necessarily distinct because $k' > 2$, $k > 2$. Label them **1, 2, 3, 4** reading clockwise about the boundary of, say, T_2 and **6, 5, 4, 3** reading clockwise about the boundary of $\mathbf{T}_1$. We wish to determine the order of these six vertices on **A**. As noted earlier, the four vertices **1, 2, 3, 4,** and also the four vertices **3, 4, 5, 6** must have that cyclic order on **A**, up to a possible reversal of orientation. Assume one of the two possible orientations on **A**

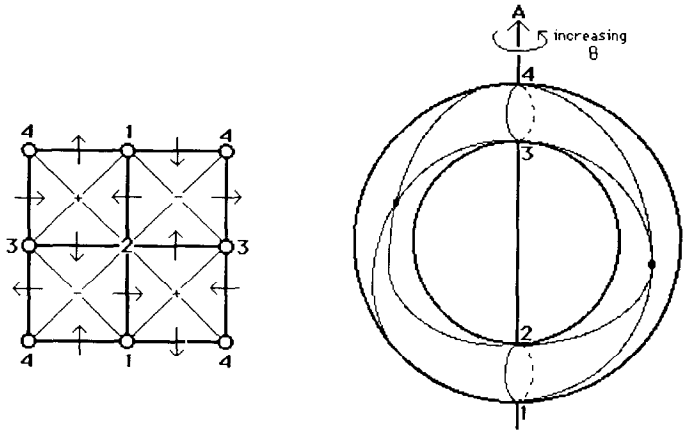

Fig. 12.

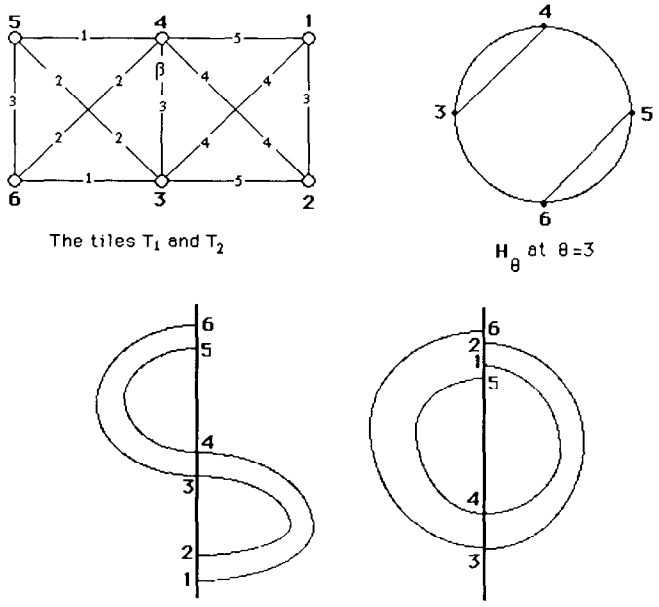

Fig. 13.

and assume that the locations of **3**, **4**, **5**, **6** on **A** have been fixed, as in the right picture in Fig. 13, which shows the axis **A** as the boundary of the disc fiber $\mathbf{H}_\theta$ at $\theta = 3$.

We ask where **1** and **2** can go? Going to the top left sketch in Fig. 13 we notice that there must be arcs $b_{56}(\theta)$, $b_{34}(\theta)$ and $b_{12}(\theta)$ joining the vertices **5** to **6**, **3** to **4**, and **1** to **2** respectively in $\mathbf{T} \cap \mathbf{H}_\theta$ at $\theta = 3$. Since $\mathbf{H}_\theta$ is a disc, this means that **1** and **2** cannot separate either **5** and **6** or **3** and **4** on $\mathbf{A} = \partial \mathbf{H}_\theta$. Going to the top right sketch in Fig. 13, let $\mathbf{A}_{ij}$ denote the subarc of the axis which lies between adjacent vertices **i** and **j** and does not contain the other two pierce points. The fact that β is innermost also shows that **1** and **2** cannot be in $\mathbf{A}_{34}$, so either **1** is in $\mathbf{A}_{45}$ and **2** is in $\mathbf{A}_{63}$ or both are in $\mathbf{A}_{45}$, $\mathbf{A}_{56}$ or $\mathbf{A}_{63}$. The second and the fourth cases are equivalent under a symmetry, so it suffices to consider the first, second and

third. However, by reversing the order of the fibration, we interchange the roles of **1**, **2** and **5**, **6**, so the first case is equivalent to the third. Thus we may assume that the points **1**, **2** are in $\mathbf{A}_{45}$ or $\mathbf{A}_{56}$. The six vertices thus have the order **1**, **2**, **3**, **4**, **5**, **6** or the order **3**, **4**, **5**, **1**, **2**, **6**, as illustrated in the two bottom sketches in Fig. 13.

Passing to Fig. 14, we consider the case where the order on **A** is **1**, **2**, **3**, **4**, **5**, **6**. We now look at the two tiles which are glued to T_1 and T_2 along the **632** edge of $T_1 \cup T_2$. Let the new vertices be **5'**, **4'**, **1'**, so that the new tiles are **65'4'3** and **34'1'2**, as in Fig. 14. The facts that there are no tile vertices between **3** and **4** on the finite part of **A**, and that the signs of the four tiles alternate checkerboard fashion, and that $k' > 2$, $k > 2$ forces the 9 vertices to be distinct and to have the order **1'**, **1**, **2**, **3**, **4**, **4'**, **5'**, **5**, **6** on **A**, as illustrated in Fig. 14. (The tiles **65'4'3** and **34'1'2** are "behind" **3456** and **4321**).

Since $k' > 2$ and $k > 2$ there must be at least one more new tile glued to T_1 along its **54** edge. Let its new vertices be **X** and **Y**, so that the new tile is **54YX**. The fact that **T** is embedded forces **X** to be between **6** and **5'** and **Y** to be between **4'** and **3**. The fact that the signs of the tiles **3456** and **54YX** are different forces **X** to be between **6** and **5** and **Y** to be between **4** and **3**. However, $\beta = \mathbf{34}$ is innermost, so that is impossible. Thus the only possibility is that $\mathbf{5} = \mathbf{5'}$, $\mathbf{4} = \mathbf{4'}$, $\mathbf{1} = \mathbf{1'}$. The case where the order of the six vertices is **3**, **4**, **5**, **1**, **2**, **6** is identical, even to the choice of the additional tiles which are glued on. Thus we have proved that **R** has dimension 2 tiles by k tiles.

How do our $2k$ tiles fit together? The fact that the signs of the singularities alternate in the tiling of **T** will be seen to place yet another restriction on the embedding, i.e. we will see that "tubes cannot go through tubes". (Remark: without this restriction it is possible to construct examples which contain tubes going through tubes, however any such example will necessarily contain adjacent tiles with singularities having the same sign.) To see this, we pass to a slightly different decomposition of **T**. Go back to the fundamental domain **R**, which is a rectangle which is 2 tiles high and k tiles wide. Choose vertical arcs $c_1, \ldots, c_k$ on **R** which run from the top edge of **R** to the corresponding point on the bottom edge, each c_i containing two singular points of the foliation. Thus each c_i is a circle on **T**. Let $A_1, \ldots, A_k$ be annular neighborhoods of $c_1, \ldots, c_k$ on **T**. Let $S_1, \ldots, S_k$ be the complementary annuli. See Fig. 15. Then each S_i is a 2-holed sphere which is pierced twice by **A** and is foliated without singularities. We may visualize the A_i's as "joining tubes" which join up the S_j's in a cycle.

We now concentrate on how a single S_i and its two joining tubes A_i and A_{i+1} are embedded in S^3. We have labeled various leaves in the foliation in Fig. 15 as occurring in

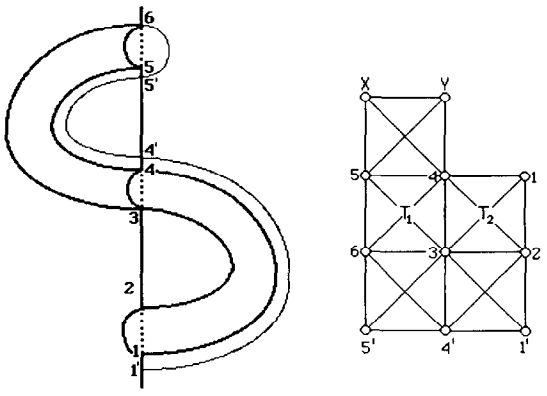

Fig. 14.

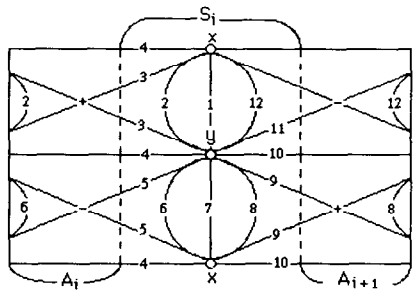

Fig. 15.

fibers at $\theta = 1, 2, 3, \ldots, 12$, also we have labeled the signs of the singularities. Figure 16 shows these same leaves as they would appear on $A_i \cup S_i \cup A_{i+1}$ in 3-space. A key point in determining the embedding is the checkerboard arrangement of these signs.

We now have a standard "template" from which we can construct the entire embedding of **T**. The embedding is determined by the embedding of our standard template. Continuing the construction of **T** in this manner we see that each A_i can be thought of as the boundary of a regular neighborhood of an arc α_i contained in a disc fiber $\mathbf{H}_{\theta_i}$. Furthermore, the manner in which copies of the template are glued together (see the example in Fig. 17) guarantees that these arcs are pairwise disjoint. That is, **T** has a type **k** embedding. ‖

§3. TORI WHICH ADMIT MIXED FOLIATIONS

In this section we concern ourselves with mixed foliations. Recall that a mixed foliation will have both type **bb** and type **bc** singularities. We say that a mixed foliation is *standard* if all of its singularities are type **bc**.

LEMMA 9. *Assume that* **T** *is a torus in the complement of a closed braid, and that* **T** *has a mixed foliation. Then, after a sequence of exchanges we may assume that* **T** *has a standard mixed foliation.*

Proof. The proof will be similar to the proof of Lemma 7, but it will be more complicated. Since a mixed foliation does not naturally give rise to a cellular decomposition of **T**, we must construct one.

The first thing to notice is that **bc**-annuli must occur in pairs, because the **c**-circle boundary component of a **bc**-annulus can only be attached to **c**-circle boundary component of another **bc**-annulus. Now, consider the annulus, W, which is constructed by attaching two **bc**-annuli together along their **c**-circle boundary component, as in the top picture in Fig. 18. Each component of ∂W is the union of two **b**-arcs and contains two points of $\mathbf{A} \cap \mathbf{T}$. We now cut W open along two new disjoint edges, e and e', each having its endpoints at points of $\mathbf{A} \cap \mathbf{T}$ which are on distinct components of W, as in the bottom picture in Fig. 18. We see that W is the union of two **be**-tiles where the boundary of **be**-tile has two **b**-arcs and two of the new **e**-arcs. Notice that the number of **be**-tiles constructed in a mixed foliation is exactly equal to the number of **bc**-annuli. The vertices in the **be**-tiling are the points of $\mathbf{A} \cap \mathbf{T}$.

We now have a cellular decomposition on **T** where the 0-cells are the points of $\mathbf{A} \cap \mathbf{T}$, the 1-cells are **b**-arcs and **e**-arcs, and the 2-cells are **bb**-tiles and **be**-tiles. Let V be the number

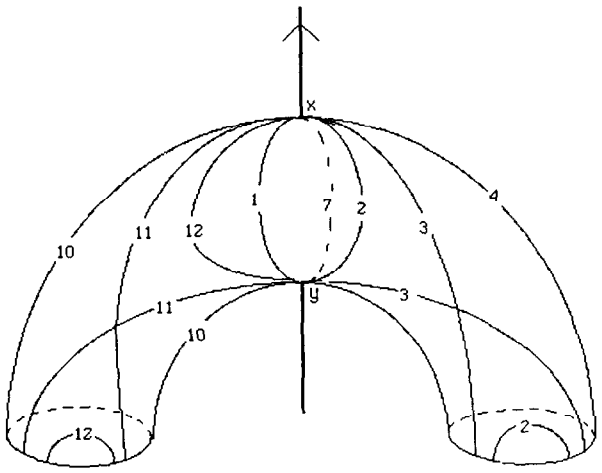

Fig. 16.

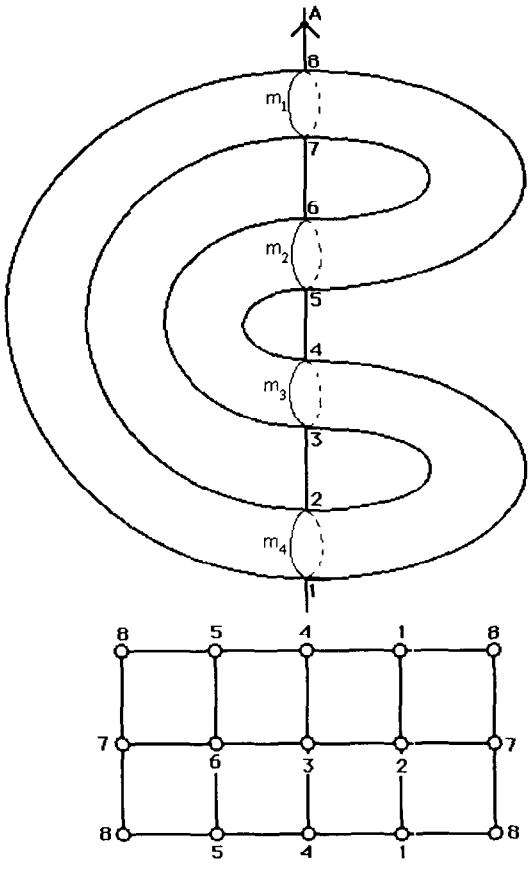

Fig. 17.

of 0-cells, E the number of 1-cells, and R the number of 2-cells. Then $V - E + R = 0$. As before, since each 2-cell has four 1-cells and every 1-cell is adjacent to two 2-cells we know $2R = E$. As before, V and E are related by $2V - E = 0$. We could easily obtain an analog of equation (1), but we need something more, because we have two kinds of edges, **b**-edges and

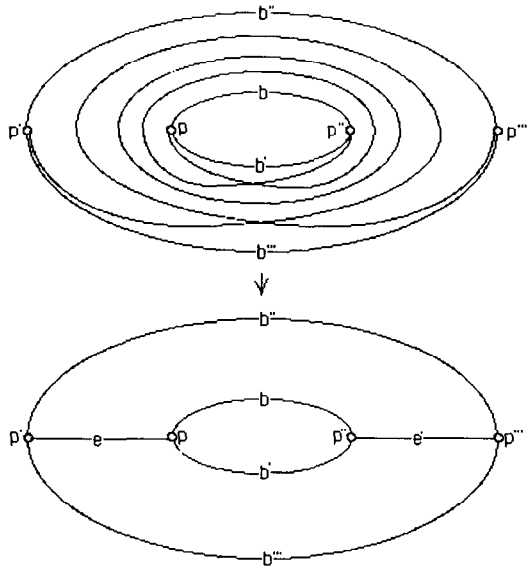

Fig. 18.

e-edges, and need to distinguish between them in our count. Let $V(\beta, \varepsilon)$ be the number of 0-cells in the tiling of **T** which have β **b**-arcs and ε **e**-arcs incident to them. Let i be the valence of a 0-cell. Then $\beta + \varepsilon = i$, so that $V(\beta, i - \beta)$ denotes the number of 0-cells of **T** which have valence i and have β **b**-arcs as 1-cells. Notice that $i - \beta$ is at most β in the expression $V(\beta, i - \beta)$, because **b**-arcs and **e**-arcs alternate around the boundary of a **be**-tile, and a **bb**-tile contains only **b**-arcs in its boundary. Thus, $i \leq 2\beta \leq 2i$ or $[i/2] \leq \beta \leq i$. Thus $V(i)$ is the sum of all $V(\beta, i - \beta)$, as β varies between $[i/2]$ and i. Therefore the analog of equation (1) is:

$$2V(2,0) + 2V(1,1) + V(2,1) + V(3,0) = \sum_{i=5}^{\infty} \sum_{\beta=[i/2]}^{i} (i-4)V(\beta, i-\beta) \tag{2}$$

where as before both the left hand side and the right hand side are non-negative.

We now claim that $V(1,1) = 0$. For, suppose not. Then there is a vertex which is incident to a single **b**-arc and a single **e**-arc. This can happen only if there is a **bc**-annulus J which has both of its **b**-arc boundary edges identified in the foliation. Let c be the **c**-circle boundary component of J which is contained in a fiber $\mathbf{H}_\theta$ of **H**. Let d_c be the subdisc in $\mathbf{H}_\theta$ which c bounds. Notice that d_c is punctured by **L**, and the number of such punctures is algebraically non-zero. Construct the 2-sphere $J \cup d_c$. This sphere has non-zero algebraic intersection number with **L**, but that is impossible.

We also claim that $V(2,1) = 0$. If not, there is a vertex p of type (**bbe**), i.e. the three tiles which meet at p have singularities of types **b**, **b** and **e**. Let b, b' and e be the tile edges of type **b**, **b**, **e** which meet at p. Then e necessarily cuts between the two boundary components of an annulus W as in the bottom picture of Fig. 18, so b and b' must be in the situation of the edges b and b' in the bottom picture of Fig. 18. Also, since there are exactly three tiles which meet at p, and since two of them are type **be**, the third tile must be a **bb**-tile. However, a **bb**-tile has four distinct vertices, whereas b and b' have two endpoints in common, namely p and also p''. This means that the **bb**-tile would have three vertices, not four, so this cannot occur.

Suppose now that there are vertices having valence ≥ 5. Then the right hand side of equation (2) is positive, so the left hand side must be too. Since we have just proved that

$V(1,1) = V(2,1) = 0$, we conclude that either $V(2,0) > 0$ or $V(3,0) > 0$, i.e. there is a vertex of type (**bb**) or (**bbb**) in the mixed foliation of **T**. Part (i) of Lemma 6 applies. Thus **L** admits an exchange move, and after the exchange move we may reduce the complexity. This process ends when every vertex has valence 4.

By hypothesis, **T** has a mixed foliation, so **e**-edges occur. If every vertex has type (**bebe**) the mixed foliation is standard and we are done. If not, some **bb** tile must be adjacent to a **be** tile, so we may assume that there is a vertex of type (**bebb**). The vertex p in Fig. 19 illustrates the only possible picture. There are two **bb** tiles and two **be** tiles. If we now translate this configuration back to the foliation on **T** we see that p will have two **bb** tiles and one **bc** annulus attached to it, as shown in Fig. 19. By an analysis which is similar to that used in the proof of Lemma 7, we deduce that the signs of the two **bb** tiles are opposite. Thus the sign of the singularity in the **bc** annulus will agree with that in one of the **bb** tiles, as illustrated. Lemma 6 applies again. The foliated region **R** which we wish to change now is a union of a **bb**-tile and a **bc**-annulus. See Fig. 20. In the original foliation, depicted on the left, the first singularity is between **b**-arcs joining p_1 to p_4 and p_2 to p_3. After the singularity there will be a **b**-arc joining p_1 to p_2, which forms a singularity with the **c**-circle. After the change, the first singularity is between **b**-arcs joining p_2 to p_3 and the **c**-circle. This results in a new **b**-arc through p_2 and p_3, which then has a singularity with **b**-arcs which join p_1 to p_4.

After the change in foliation the vertex p_1 will have valence 2. By Lemma 6, part (ii) we may then reduce the complexity. After a finite number of such reductions we will obtain a torus which has a standard mixed foliation. ‖

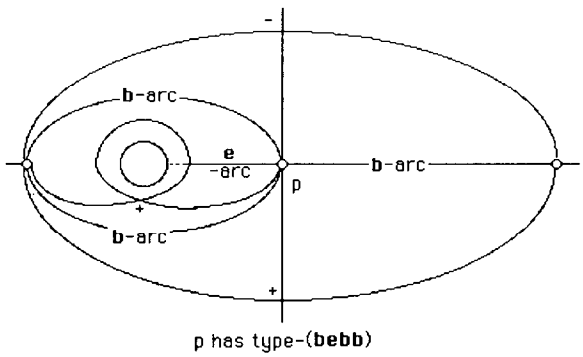

Fig. 19.

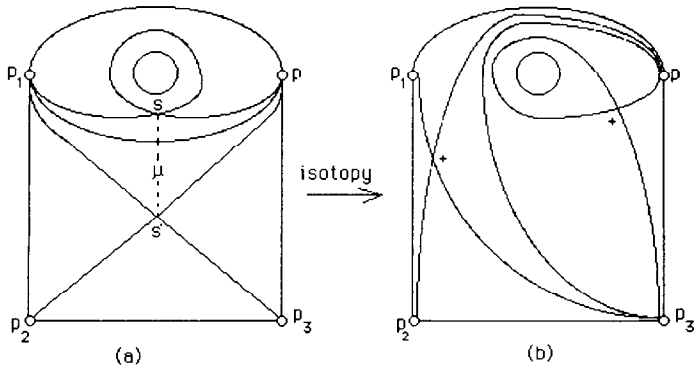

Fig. 20.

To continue, we assume that we are given a collection $\{\mathbf{T}_1,\ldots,\mathbf{T}_k\}$ of disjoint tori, each of which has a standard mixed foliation. Choose any torus $\mathbf{T}$ in the collection. Cutting $\mathbf{T}$ open along its **c**-circle boundary curves, we obtain a collection of k annular regions, each punctured twice by the braid axis, as in Fig. 21, and each containing two singularities of the foliation. Divide each such region into three concentric annuli, two of which (call them X_i and Y_i) are closest to the boundary components x_i and y_i, and are foliated without singularities by circles parallel to x_i and y_i. We choose to think of the central annulus S_i as a sphere with holes. It is foliated with two singularities at points we have labeled p_i and q_i. Choose the notation so that Y_i and X_{i+1} are adjacent on $\mathbf{T}$, and let A_i be the annulus $Y_i \cup X_{i+1}$. Then $\mathbf{T}$ is the union of the 2-*spheres* $S_1,\ldots,S_k$, each punctured twice by $\mathbf{A}$ and containing two **bc** singularities, tubed together along the *tubes* $A_1,\ldots,A_k$. The cyclic order of the spheres and tubes on $\mathbf{T}$ is $\ldots S_{i-1}, A_i, S_i, A_{i+1},\ldots$. The bottom picture in Fig. 21 shows the singular leaves in the foliation of S_i.

To understand the embeddings in 3-space, we pass to Fig. 22. The embedding of the tubes is clear, because each is foliated without singularities by **c**-circles. Thus they are embedded as braided tubes (see Fig. 22). Each tube may go around the axis several times, also distinct tubes may be braided with one-another.

As for the spheres, regard the braid axis $\mathbf{A}$ as a line in 3-space and fibers of $\mathbf{H}$ as half-planes through $\mathbf{A}$. Choose two points on $\mathbf{A}$ and declare them to be the two points **1** and **2** of $\mathbf{A} \cap S_i$. Choose distinct half-planes at, say, θ_{-1} and θ_1, and declare them to be the two fibers

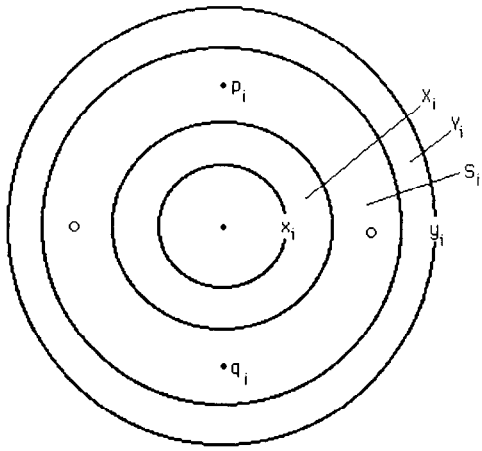

(a) Sphere-tube decomposition

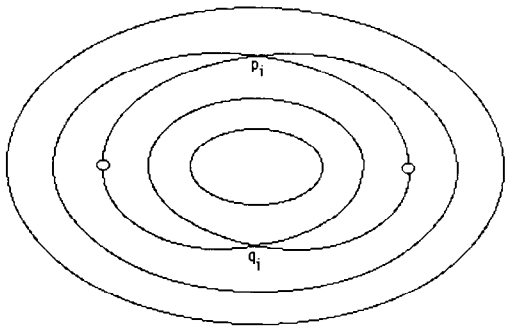

(b) Foliation of sphere-part

Fig. 21.

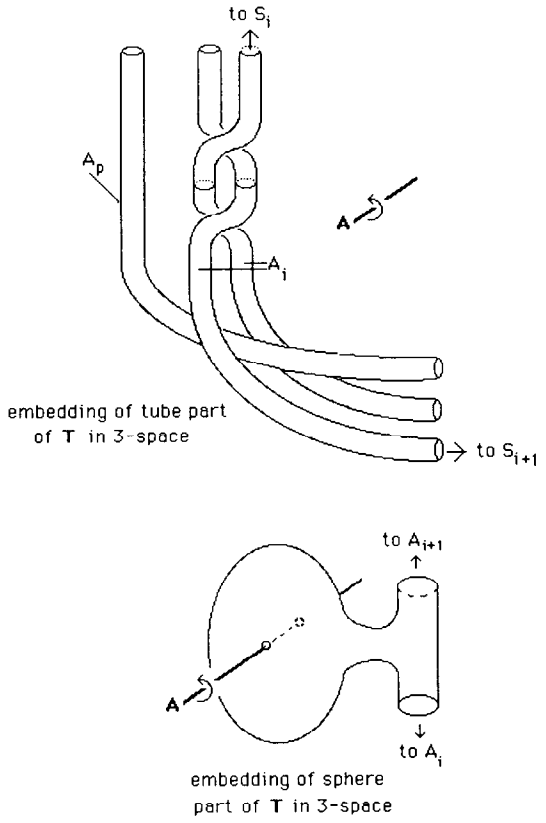

Fig. 22.

which are tangent to S_i. Join the punctures by singular leaves in these two fibers. The remaining leaves of the foliation of S_i will non-singular, and will be either be **b**-arcs joining **1** and **2** or circles. By exactly the procedure that we used in the proof of Lemma 8 we fill these in. There is essentially one way to do it, as S_i is transverse to the fibers of **H** everywhere except at θ_1 and θ_{-1}. See the bottom pictures in Fig. 22. Figure 23 illustrates an example of a torus **T** which has tubes passing through tubes. An associated $\mathbf{H}_\theta$ sequence is illustrated in Fig. 24.

LEMMA 10. *For any tube A_i, the singularities on the 2-spheres S_{i-1} and S_i which are closest to A_i have opposite signs, as in Fig.* 25.

Proof. We examine the situation in a sequence of fibers, starting just before the singularity in S_i, until just after the singularity in S_{i+1}. We use the pictures in the top row in Fig. 26 to illustrate what we wish to say. The positive **bc**-singularity at θ_{-1} results in the creation of the tube A_i. The circle which is illustrated at θ_0 is the intersection of A_i with the fiber at θ_0, and the fact that the singularity which created it was positive implies that the side of it which does not bound a disc is negative. But then the **bc**-singularity at θ_1, which annihilates the tube, must be negative. ‖

A tube A_i in the decomposition of **T** will be said to be *outermost* if, for any non-singular fiber $\mathbf{H}_\theta$ which meets A_i non-trivially the **c**-circle $\mathbf{H}_\theta \cap A_i$ is not contained in the disc bounded by $\mathbf{H}_\theta \cap A_k$ for any other tube A_k.

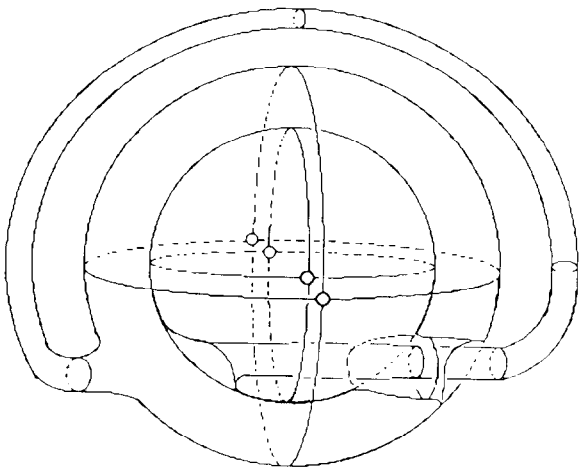

Fig. 23.

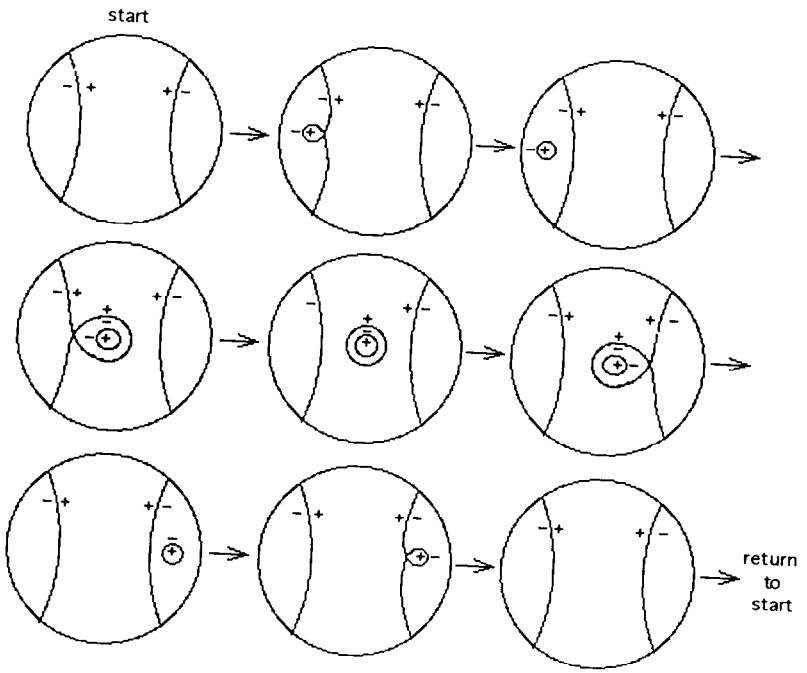

Fig. 24.

LEMMA 11. (sphere amalgamation lemma). *Choose an outermost tube A_i in the decomposition of* **T**. *Suppose that there exists a rectangular region* **R** *in all of the disc fibers between θ_{-1} and θ_1, as illustrated in the middle picture in Fig.* 26, *such that for all $\theta \in [\theta_{-1}, \theta_1]$ the link* **L** *intersects $\mathbf{H}_\theta \cap \mathbf{R}$ only inside the subdisc bounded by the* **c**-*circle which is inside* **R**. *Then after a change in fibration we may replace the* **bc**-*singularities in the fibers at $\theta_{\pm 1}$ with* **bb**-*singularities. Moreover, after the change we will have a new standard mixed foliation with fewer* **bc**-*singularities.*

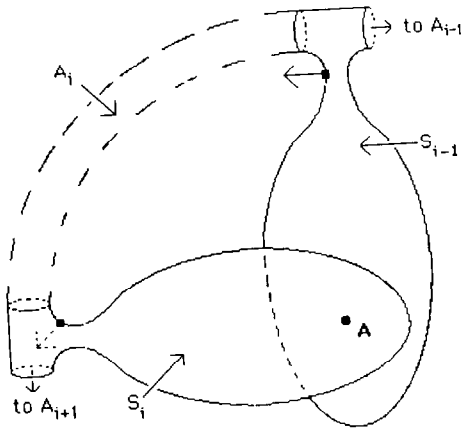

Fig. 25.

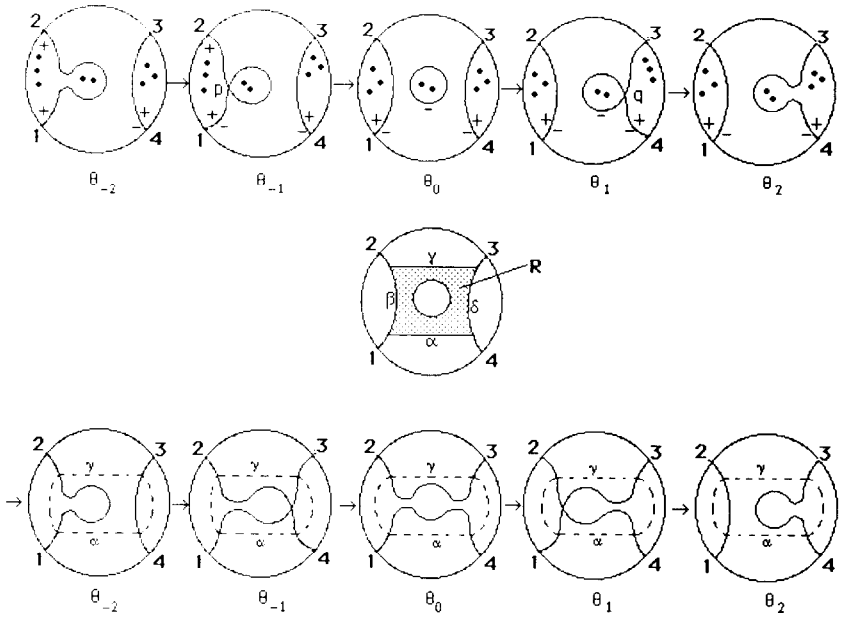

Fig. 26.

Proof. Refer to the middle diagram in Fig. 26, where the rectangular region **R** is illustrated. Its boundary is labeled $\alpha \cup \beta \cup \gamma \cup \delta$. The hypotheses of the sphere amalgamation lemma ensure that there is no obstruction to replacing the $\mathbf{H}_\theta$-sequence in the top row of Fig. 26 with the sequence in the bottom row. A careful look at that sequence shows that after the change in fibration the vertices which are labeled **1**, **2**, **3**, **4** will all have valence 2 and type **bb**. We may then use Lemma 6 to eliminate these **bb**-singularities, to produce a standard mixed foliation with fewer **bc**-singularities. ‖

LEMMA 12. (the exchange move lemma for tori with standard mixed foliations). *Let A_i be an outermost tube and let S_{i-1} and S_i be its adjacent 2-spheres. Then, after a series of*

exchange moves, we may assume that S_{i-1}, A_i, S_i satisfy the hypotheses of the sphere amalgamation lemma.

Proof. We examine the geometry of Fig. 26, but from a new point of view: instead of looking at how **L**, S_{i-1}, and S_i meet a sequence of fibers of **H**, we look at them under a regular projection onto a plane which is orthogonal to **A**. See Fig. 27. Regard S^3 as $R^3 \cup \{\infty\}$ and **A** as the z-axis $\cup \{\infty\}$. Let α_i be the core of the tube A_i, i.e. α_i is an arc in $S^3 - \mathbf{L}$ which joins the capped spheres CS_{i-1} and CS_i. Without loss of generality we may assume that the orthogonal projection π of $\mathbf{R}^3$ onto the x-y plane induces a regular projection for the link **L** and the arc α_i. We may further assume that the images $D_{i-1} = \pi(CS_{i-1})$ and $D_i = \pi(CS_i)$ are radially foliated concentric discs and that neither **L** nor α_i passes under or over D_i or D_{i-1}. Strands of **L** will, however, enter the discs, and then wind about the axis, possibly braiding as they do so. There may be other tubes A_j in the picture, but if so we may assume without loss of generality that they are arbitrarily close to the strands of **L**, because our tori are incompressible, so for simplicity we have not shown them. There may also be strands of **L** inside the tube A_i, but if so they may be assumed to be arbitrarily close to α_i, so for simplicity we have not shown them either in Fig. 27. Finally, we will simplify our picture whenever we need to do so by pushing the braiding of **L** into "boxes", as needed, so that the visible part of **L** is seen as a set of parallel strands in our projection.

We now observe that if the arc α_i lies above all of the strands of **L** in Fig. 27, then we may push it into upper half-space. The intersections of a regular neighborhood of α_i in 3-space with fibers of **H** will then give us the region **R** which was described in the sphere amalgamation lemma. In general that will not be the case. Instead, α_i will thread under and over **L** in its passage from D_{i-1} to D_i. Our problem is to eliminate that threading.

In order to get a measure of the complexity of the threading of our arc α_i, we now lift D_{i-1} and D_i a little bit out of the plane of projection, so that they are seen as disjoint discs

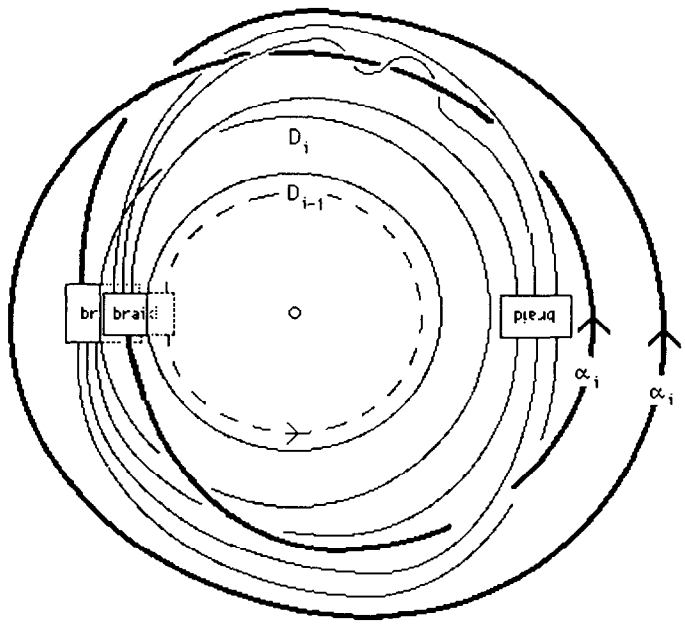

Fig. 27.

above and parallel to the projection plane. This "lifting" of D_{i-1} and D_i will lift the endpoints of α_i out of the projection plane, so that now α_i starts at ∂D_i, above the plane of projection, and then (as it crosses under **L**) it will be forced to dip down, puncturing the projection plane. We assume that it dips up and down, puncturing the plane transversally each time, until it ends at ∂D_i. Without loss of generality we may assume that the punctures occur away from the braid boxes. See Fig. 28. Define the *complexity* $C(\alpha_i)$ to be the number of points of intersection of α_i with the x-y plane. By our earlier observation, if we can find moves which reduce $C(\alpha_i)$ the lemma will be proved.

Our first move is a *rotation* of D_{i-1}, as illustrated in Fig. 29. We have not shown D_i in this picture, however we have added the braid box which is inside D_{i-1} and the corresponding strands of **L**. The purpose of the rotation (look ahead to Fig. 30) is to create an interval in the polar angle function belonging to the braid box which is inside D_{i-1} which is disjoint from the corresponding braid box inside D_i. As a result of the rotation the portion of **L** which is out of the plane of projection and attached to ∂D_{i-1} will be lengthened, while the corresponding portion of α_i (and all parts of **L** and other tubes which are close to α_i) will be shortened. Rotating D_{i-1} does not change $C(\alpha_i)$.

Our next move is an *exchange move*, illustrated in Fig. 30. The capped 2-sphere which we are calling D_{i-1} is pulled across the axis, taking the part of the link which is inside it across the axis as it goes, and pulled through **L**, and then back across the axis. The orders of D_{i-1} (which is illustrated) and D_i (which is not) will be switched. This will in general introduce new braiding in **L**, as illustrated. However, the important feature is that after the exchange move we will be able to isotope α_i so that it has one less puncture with the x-y plane.

After a finite number of rotations and exchange moves we will have $C(\alpha_i) = 0$, and $S_{i-1} \cup A_i \cup S_i$ will satisfy the hypotheses of the sphere amalgamation lemma. ‖

After applying Lemmas 11 and 12 as often as necessary, we will have replaced our torus **T** by a new embedded torus which has a standard mixed foliation and exactly one 2-sphere and one tube, that is it has a type **1** embedding. ‖

§4. THE PROOF OF THEOREM 1, COROLLARIES 1 AND 2 AND THEOREM 2

Proof of Theorem 1. By hypothesis, we are presented with a finite collection $\Omega = \{\mathbf{T}_1, \ldots, \mathbf{T}_q\}$ of tori in $S^3 - \mathbf{L}$, where the ith torus $\mathbf{T}_i$ has a foliation whose type can be altered to type $\varepsilon_i = 0$, 1 or k. The key to the proof is to do the modifications which we introduced earlier in a controlled order.

By Lemma 4 we may assume that every torus has a circular foliation, a mixed foliation or a tiling. Also, we may assume that if the foliation is circular then the embedding is type **0**.

The modifications which were used to alter the tori $\mathbf{T}_i$ with $\varepsilon_i = 1$ and $k \geq 2$ were described in Lemmas 6, 7, 8, 9, 11 and 12. They used four different modifications:

Modification (i): Isotopy of 3-space;

Modification (ii): Change in the fibration **H**, predicated on the existence of two adjacent **bb**-tiles having the same parity;

Modification (iii): An exchange move and elimination of a valence 2 vertex, if such a vertex exists;

Modification (iv): An exchange move and rotation, as in Lemma 12.

Modification (i) does not change the embedding types of any of our tori. Modification (ii) alters the foliation of two **bb** tiles, but leaves everything fixed outside an arbitrarily small

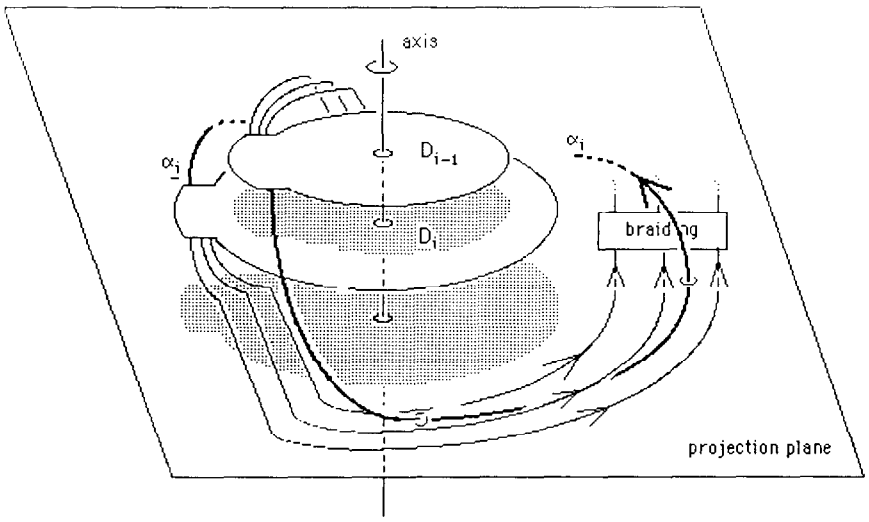

Fig. 28.

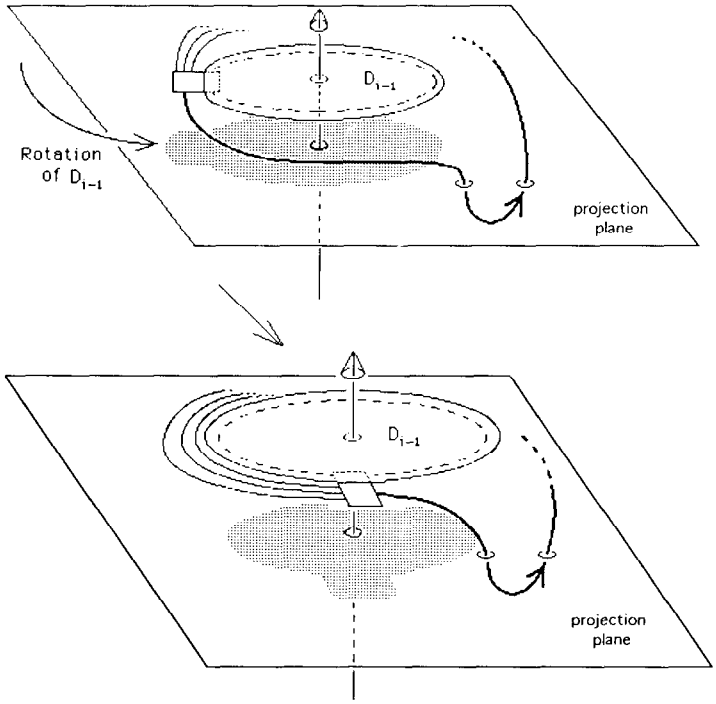

Fig. 29.

neighborhood of these tiles. Modification (iii) alters the foliation in a neighborhood of the valence 2 vertex which is being eliminated, but leaves everything outside a small neighborhood of this vertex unaltered. Modification (iv) changes the embedding of the tori of type **1** and **k**, but not of a torus of type **0**. We used modifications (i), (ii) and (iii) in standardizing the embedding of the tori of type **k**. We used all four modifications in standardizing the embedding of the tori of type **1**.

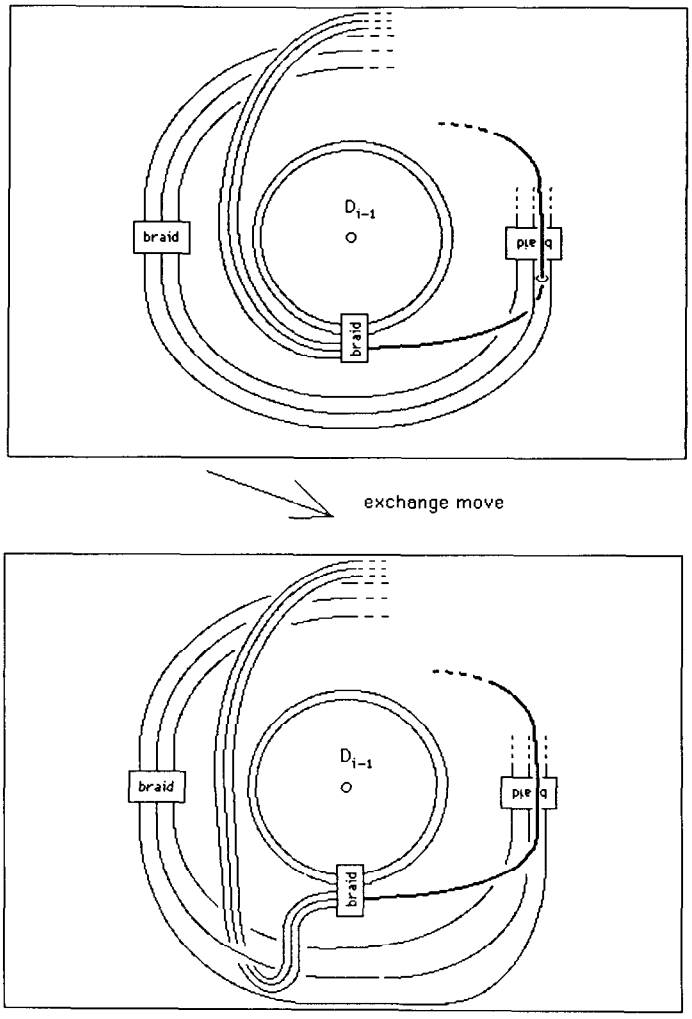

Fig. 30.

As noted earlier, to begin we assume that every torus has a type **0** embedding or has a mixed foliation or a tiling. Applying the four modifications as often as necessary (using Lemmas 9, 10, 11, 12) we may assume that every T_i with $\varepsilon_i = 1$ has an embedding of type **1**. Notice that if there were tori which admit tilings, then after the modifications they will continue to admit tilings, however the tilings themselves may change. Using Lemmas 4, 6 and 7 we then go to the tori $\mathbf{T}_i$ with $\varepsilon_i = k$, and standardize their tilings. By Lemma 8 we conclude that every torus of type $\varepsilon_i = k$ will then have a type **k** embedding. The modifications used in Lemmas 4, 6 and 7 are (i)–(iii) of the above list. These modifications only alter the foliation of the tori locally, i.e. within two **bb**-tiles for operation (i) and within a neighborhood of a valence 2 vertex for operation (ii). Therefore they will not disturb the embeddings of type **0** and **1**. The proof of Theorem 1 is complete. ‖

In the Introduction we stated two results (Corollaries 1 and 2) which give detailed information about the closed braid representatives of non-simple links of braid index 3 and 4. We are now ready to prove them.

Proof of Corollary 1. We are given a non-simple link **L** of braid index 3. Choose a closed 3-braid structure for **L**. Let **T** be the essential, non-peripheral torus in $S^3 - \mathbf{L}$. By Theorem 1 we may assume that **T** has an embedding of type **0**, **1** or **k** relative to the half-planes $\{\mathbf{H}_\theta; \theta \in [0, 2\pi]\}$ in our braid structure. Choose a non-singular fiber $\mathbf{H}_\theta$ of **H**. Our link **L** will intersect $\mathbf{H}_\theta$ in 3 points, which we refer to as "dots". We examine $\mathbf{T} \cap \mathbf{H}_\theta$ when **T** has a type **0**, **1** or **k** embedding. The reader may find it helpful to consult Fig. 6, which depicted $\mathbf{T} \cap \mathbf{H}_\theta$, as viewed on **H**, in the three cases.

Our first claim is that **T** cannot be type **k** with $k \geq 2$. For, suppose that it was. The intersections of **T** with $\mathbf{H}_\theta$ will consist entirely of **b**-arcs and there are $k \geq 2$ of them, with $2k$ endpoints on $\mathbf{A} = \partial \mathbf{H}_\theta$. We study them, as they evolve in the cycle of fibers $\{\mathbf{H}_\theta; 0 \leq \theta \leq 2\pi\}$. Each **b**-arc must eventually be surgered, and during the cycle there are exactly four singular arcs which emanate from each point of $\mathbf{A} \cap \mathbf{T}$.

Assume first that $k = 2$. There are 4 points in $\mathbf{A} \cap \mathbf{T}$ and there are two **b**-arcs in each non-singular fiber. Choosing a non-singular fiber $\mathbf{H}_\theta$, we see two **b**-arcs with their endpoints on the axis **A**. Let us suppose that the notation is chosen so that the points in $\mathbf{A} \cap \mathbf{T}$ are **1**, **2**, **3**, **4** and that $b_{12}(\theta)$ and $b_{34}(\theta)$ are the **b**-arcs in that fiber, where b_{ij} joins **i** to **j**. They divide the fiber into two half discs $d_{12}(\theta)$ and $d_{34}(\theta)$ and a half annulus $A(\theta)$ and there must be a dot in each half-disc because if not our **b**-arcs would be inessential. That means that there is at most one dot in $A(\theta)$. But then, after the first surgery we will have new **b**-arcs $b_{14}(\theta')$ and $b_{23}(\theta')$, which divide $\mathbf{H}_\theta$ into two half-discs and a half-annulus, and on of the discs will not contain a dot. Thus there will be an inessential **b**-arc. Hence type **k** is impossible for $k = 2$, and therefore even more so for $k > 2$.

We rule out the occurrence of a mixed foliation on slightly different grounds. If there is a **bc**-annulus in the foliation of **T**, then the **c**-circle associated with this annulus must be essential. It therefore bounds a subdisc d_c of $\mathbf{H}_\theta$ which contains one of the three points of $\mathbf{H}_\theta \cap \mathbf{L}$. If we surger **T** along d_c, we produce an essential twice punctured 2-sphere. But then, **L** must represent a composite link, contradicting the assumption that **L** is prime. Therefore **T** must have a standard circular foliation. The description of **L** follows immediately, because there are only three braid strands. ‖

Proof of Corollary 2. We proceed as in the proof of Corollary 1, only now our link **L** will intersect each $\mathbf{H}_\theta$ in 4 points. We examine $\mathbf{T} \cap \mathbf{H}_\theta$ when **T** has a type **0**, **1** or **k** embedding.

Type **0**. Notice that $\mathbf{T} \cap \mathbf{H}_\theta$ contains at most two c-circles. Each bounds a disc which contains at least one dot. Thus there are three cases:

Case 1. There are two discs, each containing two dots. This gives the 4-braid $(\sigma_1)^p(\sigma_3)^q(\sigma_2\sigma_1\sigma_3\sigma_2)^r$, where the factors $(\sigma_1)^p$ and $(\sigma_3)^q$ correspond to braiding inside the discs and the factor $(\sigma_2\sigma_1\sigma_3\sigma_2)^r$, corresponds to a knotting of the torus by braiding between the two discs. *Case* 2. There is one disc d. It contains three dots. The fourth dot is in $\mathbf{H}_\theta - d$. This gives the 4-braid $\beta(\sigma_3\sigma_2\sigma_1^2\sigma_2\sigma_3)^p$. The braid β corresponds to braiding among the three dots inside d. The factor $(\sigma_3\sigma_2\sigma_1^2\sigma_2\sigma_3)^p$ represents a winding of the fourth strand around the outside of the unknotted solid torus. *Case* 3. There is one disc d which contains two dots. The other two dots are in $\mathbf{H}_\theta \setminus d$. The braid is $(\sigma_2)^p(\sigma_1\sigma_2^2\sigma_1)^q(\sigma_3\sigma_2^2\sigma_3)^r$. The factor $(\sigma_2)^p$ comes from braiding inside the disc. The factors $(\sigma_1\sigma_2^2\sigma_1)^q$ and $(\sigma_3\sigma_2^2\sigma_3)^r$ represent separate windings of the remaining two strands about the unknotted torus **T**.

Type **1**. The intersections of **T** with **H** consist of a single **b**-arc and some number of **c**-circles. The arc cuts off a half-disc h in $\mathbf{H}_\theta$ which contains at least one dot. The circles each bound discs, and each disc contains at least one dot, also the same number of dots are in each disc. There also may be dots outside h and all the discs. The total number of dots is 4.

This shows that there cannot be more than one disc, for if there were two, there could only be one braid strand in each, but then **T** would be peripheral. This shows that **T** is unknotted, so there must be a dot outside h and d, leaving at most two dots inside d. However d must contain at least 2 dots, for if it only contained 1 then **T** would be peripheral. Thus the only possibility is the braid $\beta(\sigma_1\sigma_2^2\sigma_1)^p$, where the fourth strand winds about the axis inside the sphere, the middle two are inside the tube, and the factor $(\sigma_1\sigma_2^2\sigma_1)^p$ corresponds to the first strand wrapping about the middle two, to make **T** incompressible.

Type **k**. The intersections of **T** with $\mathbf{H}_\theta$ consist entirely of **b**-arcs and there are $k \geq 2$ of them, with $2k$ endpoints on $\mathbf{A} = \partial\mathbf{H}_\theta$. We study them, as they occur in the cycle of fibers $\{\mathbf{H}_\theta;\ 0 \leq \theta \leq 2\pi\}$. As in the case of 3-braids each **b**-arc must eventually be surgered, and during the cycle there are exactly four singular arcs which emerge from each point of $\mathbf{A} \cap \mathbf{T}$.

Assume first that $k = 2$. We will show that we obtain the example depicted earlier in Fig. 3. Since $k = 2$, there are 4 points in $\mathbf{A} \cap \mathbf{T}$ and there are two **b**-arcs in each non-singular fiber. Choosing a non-singular fiber at θ_1, let us suppose that the notation is chosen so that the points in $\mathbf{A} \cap \mathbf{T}$ are **1**, **2**, **3**, **4** and that $b_{12}(\theta_1)$ and $b_{34}(\theta_1)$ are the **b**-arcs in that fiber, where b_{ij} joins **i** to **j**. They divide the fiber into two half discs $d_{12}(\theta_1)$ and $d_{34}(\theta_1)$ and a half annulus $A(\theta_1)$ and there must be a dot in each half-disc because if not our **b**-arcs would be inessential. There must also be two dots in $A(\theta_1)$ for if not then after the first surgery we would obtain an inessential **b**-arc. Braiding can occur between the two dots in $A(\theta_1)$ between adjacent surgeries. After the first surgery we will have new **b**-arcs $b_{14}(\theta)$ and $b_{23}(\theta)$, which again divide $\mathbf{H}_\theta$ into two half-discs, each containing a dot, and a half-annulus containing two dots, and again there can be braiding. Continuing in this way we obtain blocks of elementary braids $(\sigma_{13})^p(\sigma_{24})^r(\sigma_{13})^q(\sigma_{24})^s\ldots$. However, there must be exactly four syllables because each block of braidings occurs during the θ-values between two adjacent singularities, and there are exactly four singular leaves emerging from each of the points **1**, **2**, **3**, **4** of $\mathbf{A} \cap \mathbf{T}$. Thus the only possibility is the 4-braid $(\sigma_{13})^p(\sigma_{24})^r(\sigma_{13})^q(\sigma_{24})^s$.

The case $k > 2$ is ruled out for the same reasons as were used to rule out the case $k = 2$ for 3-braids, i.e. it is impossible because there will necessarily be an inessential **b**-arc. ‖

In Theorem 1 we studied special positions for the torus **T** in $S^3 - \mathbf{L}$, relative to the braid axis **A** and the fibers of **H**. The fact that **T** is an embedded torus in S^3 implies that **T** bounds a solid torus **V** on at least one side. Theorem 2 asserts that, in each of the three types of embeddings, there is a natural way to describe the inclusions of $\mathbf{L} \cap \mathbf{V}$ and $\mathbf{A} \cap \mathbf{V}$ in **V**. See the Introduction for the precise statement.

Proof of Theorem 2. In the case of type **0** embeddings each **c**-circle $c(\theta)$ lies in both **T** and some fiber $\mathbf{H}_\theta$, and so bounds a disc $\mathbf{d}_c(\theta)$ in $\mathbf{H}_\theta$. The number p of such discs in $\mathbf{H}_\theta$ is independent of θ, as is the number q of points of intersection of **K** with a single disc. The union of the $\mathbf{d}_c(\theta)$'s thus spins out a p-strand braided solid torus **V**, $p \geq 1$, as θ is varied between 0 and 2π, and **K** is a closed w_0-braid inside **V**. The axis **A** does not meet **V**. The solid torus **V** is as depicted in Fig. 5.

In the situation of type **1** embeddings we study a sequence of fibers $\mathbf{H}_\theta$ of **H** to understand how $\mathbf{L} \cap \mathbf{V}$ is situated in **V**. See Fig. 31. The first picture shows a typical non-singular fiber $\mathbf{H}_\theta$ of **H**. Its intersections with **T** will be one **b**-arc and some number of **c**-circles $c_1,\ldots,c_p$, the number corresponding to the number of times the single tube wraps around the axis **A**. Each non-singular **c**-circle c bounds a disc $\mathbf{d}_c(\theta)$ in $\mathbf{H}_\theta$ and the **b**-arc bounds a half-disc $h_b(\theta)$. The links meets all of these, for if not there would be inessential **c**-circles and an inessential **b**-arc. The solid torus **V** is swept out by the $h_b(\theta)$ and $d_{c_1}(\theta),\ldots d_{c_p}(\theta)$ as θ varies over the interval $[0, 2\pi]$. Notice that as we push $\mathbf{H}_\theta$ forward in the

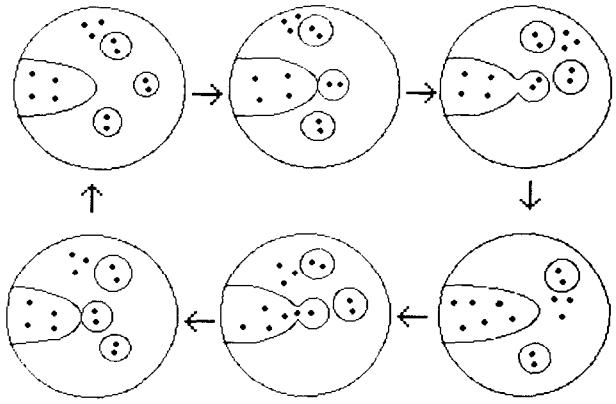

Cycle of fibers for type 1 embedding

Fig. 31.

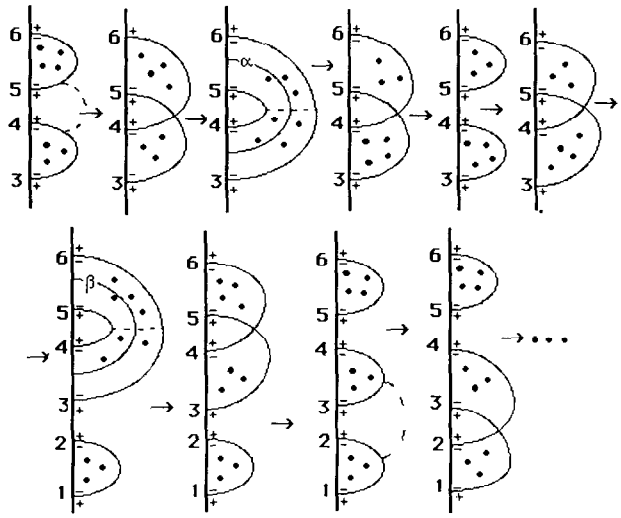

Part of H_θ sequence for type k embedding

Fig. 32.

fibration the discs $\mathbf{d}_c(\theta)$ may move around each other, creating a braided tube. Thus **V** is a 3-ball with a (possibly braided) handle attached to it. The axis **A** meets the 3-ball part of **V** in a single arc.

The **b**-arc and **c**-circles separate the points of $\mathbf{L}' \cap \mathbf{H}_\theta$ into sets such that as θ increases braiding only occurs between points of $\mathbf{L}' \cap \mathbf{H}_\theta$ which are in the same set. The only values of θ at which points in different sets are allowed to braid is between the two occurrences of **bc** singularities. It is clear that all of the braiding in this part of the cycle can be pushed into a single block. Thus we obtain the picture given in Fig. 5.

If it should happen that $\mathbf{V}' = S^3 - \mathbf{V}$ is unknotted, the identical argument gives a symmetric picture for the inclusion $(\mathbf{L} \cup \mathbf{A}) \cap \mathbf{V}'$ in $\mathbf{V}'$ in the case of a type **1** embedded torus.

To understand **L** in the situation of type **k** embeddings, $k \geq 2$, we look at that part of the $\mathbf{H}_\theta$ sequence which is associated to the foliation of a single annulus A_i and parts of its adjacent 2-spheres. Figure 32 shows two **b**-arcs, and we follow them in a sequence of fibers of **H** which includes a " + " singularity followed by a " − " singularity. At first we will see two subsets of $\mathbf{L} \cap \mathbf{H}_\theta$, where each is contained in a region which one of the **b**-arc splits off in

$\mathbf{H}_\theta$. Braiding can occur, but only between the arcs in each set. After the " + " singularity the two subsets of $\mathbf{L} \cap \mathbf{H}_\theta$ will merge into a single region of $\mathbf{H}_\theta - (\mathbf{T} \cap \mathbf{H}_\theta)$. It will then be possible to have braiding between the two sets. After the subsequent " − " singularity the points of $\mathbf{L} \cap \mathbf{H}_\theta$ contained in this single region will break up into subsets again.

The solid torus $\mathbf{V}$ is a union of the 3-balls swept out by the regions bounded by the $\mathbf{b}$-arcs, joined up by tubes, where the core of each tube lies in a single fiber. There will be k 3-balls, each meeting $\mathbf{A}$ in a single arc. There will be a block of braids associated to each 3-ball, and another block associated to the connecting annulli, but we may amalgamate them as in Fig. 5. Our proof is complete. ‖

Acknowledgements—The applications of our work to companionship were suggested by a question asked by the referee, whom we thank for stimulating us to think about this special case. We also thank Daniela Renate Hass, who as an MA student at SUNY Buffalo had the geometric insight to realize that a single 2-sphere and annulus suffice in the case of type 1 embeddings. Lemmas 10, 11 and 12 are based upon that insight.

REFERENCES

1. D. BENNEQUIN: Entrelacements et equations de Pfaff, *Asterisque* **107–108** (1983), 87–161.
2. J. BIRMAN and W. MENASCO: Studying links via closed braids IV: Split and composite links, *Invent. Math.* **102** (1990), 115–139.
3. W. H. JACO and P. B. SHALEN: Seifert fibered spaces in 3-manifolds, *Memoirs AMS*, **21**, (1979) Num. 220.
4. K. JOHANSSON: Equivalences d'homotopie des variétés de dimension 3, *C.R. Acad. Sc. Paris*, **66** (1975), 1009–1010.
5. D. ROLFSEN: *Knots and Links*, Publish or Perish, (1974).
6. H. SCHUBERT: Knoten und Vollringe, *Acta Math.* **90** (1953), 131–226.
7. W. THURSTON: On the geometry and topology of 3-manifolds, *Lecture notes*, Princeton Univ., (1982), unpublished.
8. S. YAMADA: The minimum number of Seifert circles equals the braid index of a link, *Inv. Math.* **80** (1987), 347–356.

Department of Mathematics
Columbia University
New York, N.Y. 10027
U.S.A.

Department of Mathematics
University at Buffalo
Buffalo, N.Y. 14222,
U.S.A.

Added in proof.

After this manuscript went to press our tireless referee requested additional clarification of the formula $b(L) = w_1 + \cdots + w_k$ of Corollary 3. The point which troubled the referee was that the integers $w_1, \cdots, w_k$, and thus the braid index $b(L)$ of the non-simple knot L, did not appear to depend upon the manner in which the solid torus V_c is embedded in 3-space. However, that is a misinterpretation of $w_1, \cdots, w_k$.

The example which is given in Fig. 7 and 8 may help in understanding the situation. The knot L in Fig. 7 is a double of the trefoil C, which is depicted in Fig. 8 as a union of 5 planar arcs, each of which begins and ends on A. Notice that the embedding of C which is given in Fig. 8 was chosen so that its double L would be a closed braid with respect to A. However that is not all; in addition, L must lie inside a solid torus neighborhood V_c of C and the solid torus V_c must be positioned (using the main results in this paper) to exhibit the fact that its boundary T_c is a type 5 torus.

This example illustrates the general situation. The numbers $w_1, \cdots, w_k$ depend upon inter-related phenomena, i.e. the way in which L is embedded in V_c, and the way in which A meets V_c. The facts that (i) L is a closed braid with respect to A, and (ii) L lies inside a solid torus neighborhood V_c of its companion C, and (iii) ∂V_c has a type k embedding, combine to place inter-related constraints on the integers $w_1, \cdots, w_k$. Thus $b(L)$ does, in fact, depend upon both the embedding of L in V_c and the embedding of C in 3-space.